Pergamon

Computers Math. Applic. Vol. 34, No. 2-4, pp. 195-227, 1997

0898-1221/97 $17.00 + 0.00

PII: S0898-1221(97)00124-7

Quasiattractors and Homoclinic Tangencies

S. V. GONCHENKO, L. P. SHIL'NIKOV AND D. V. TURAEV
Research Institute for Applied Mathematics and Cybernetics
10 Ul'janova st., Nizhny Novgorod, 603005, Russia

Abstract—Recent results describing nontrivial dynamical phenomena in systems with homoclinic tangencies are represented. Such systems cover a large variety of dynamical models known from natural applications and it is established that so-called quasiattractors of these systems may exhibit rather nontrivial features which are in a sharp distinction, with that one could expect in analogy with hyperbolic or Lorenz-like attractors. For instance, the impossibility of giving a finite-parameter complete description of dynamics and bifurcations of the quasiattractors is shown. Besides, it is shown that the quasiattractors may simultaneously contain saddle periodic orbits with different numbers of positive Lyapunov exponents. If the dimension of a phase space is not too low (greater than four for flows and greater than three for maps), it is shown that such a quasiattractor may contain infinitely many coexisting strange attractors.

Keywords—Attractor, Homoclinic bifurcations, Dynamical models.

1. INTRODUCTION

The discovery of dynamical chaos is one of the main achievements in the modern science. At the aftermath, various phenomena in natural sciences and engineering have obtained an adequate mathematical description within the framework of differential equations. From the mathematical point of view, dynamical chaos is commonly associated with the notion of *a strange attractor*—an attractive limit set with the complicated structure of orbit behavior.

By now, there does not exist a commonly accepted definition for a strange attractor describing dynamical chaos in real systems. Frequently, a strange attractor is regarded as a nontrivial attractive set which is composed by *unstable orbits* and which is transitive. There exist two types of attractors which correspond completely to this definition: these are hyperbolic attractors and Lorenz attractors (the latters are also called quasihyperbolic attractors). Hyperbolic attractors are structurally stable (they satisfy to Smale's "axiom A"). Lorenz attractors are structurally unstable and, moreover, they compose open sets in the space of dynamical systems. The structural instability of Lorenz attractors is connected with the fact that such an attractor contains a saddle equilibrium state together with its unstable separatrices which can form homoclinic loops of different types when parameters vary. Nevertheless, the property of transitivity and the property of instability of individual orbits are preserved by perturbations, and Lorenz attractors are similar to hyperbolic attractors with this point of view.

The "transitivity" and "instability" properties give a possibility of rigorous description of dynamical chaos in hyperbolic and quasihyperbolic systems by tools of the ergodic theory. Therefore, such attractors were called *stochastic attractors*.

This work was supported by EC-Russia Collaborative Project ESPRIT-P9282-ACTCS, by the INTAS Grant No. 93-0570 ext. and by the Russian Foundation of Fundamental Researches, Grant No. 96-01-01-135.

Typeset by AMS-TEX

However, it is necessary to remark that there are no examples (known to the authors) of dynamical models from applications where nontrivial hyperbolic attractors are found; and to the present time, the study of such attractors is the subject of the pure mathematics rather than of the nonlinear dynamics. Quasihyperbolic attractors do occur in applications but in a limited class of problems.

At the same time, for most of known dynamical systems of natural origination that demonstrate chaotic behaviour nontrivial attractive sets have quite different nature. We mention, for instance, spiral attractors [1–3] associated with a homoclinic loop to a saddle-focus [4,5]; attractors that arise through breakdown of an invariant torus [6–9]; screw-like attractors in the Chua circuit [10,11]; attractors in the Hénon map [12–14]; attractors forming through the period-doubling cascade in strongly dissipative maps; attractors in the Lorenz model

$$\dot{x} = \sigma(y - x), \qquad \dot{y} = rx - y - xz, \qquad \dot{z} = -bx + xy,$$

at large values of r (for instance, at $\sigma = 10$, $b = 8/3$, $r > 31$) [15–17]; attractors in periodically forced self-oscillatory systems with one degree of freedom [18–21], etc.

Strange attractors of such systems are well known to contain not only nontrivial hyperbolic sets but also attractive periodic orbits, and thereby, not being stochastic rigorously speaking. Due to this reason, we will adhere to the definition given in [6,22]: a strange attractor (*a quasiattractor* in terms of [6,22]) is an attractive limit set which contains nontrivial hyperbolic subsets and which may contain attractive periodic orbits of extremely long periods. Since neither the transitivity property nor the property of individual instability of orbits may not be fulfilled in this case[1] we will use the term *a quasistochastic attractor*.

We notice that the principal reason of distinguishing the class of quasistochastic attractors is that, in contrast with the genuine stochastic attractors, for them there is no rigorous mathematical base for the main notions by using of which chaotic dynamics is analyzed: Lyapunov exponents, entropy, decay of correlations, sensitive dependence on initial data, etc. Thus, for a large variety of dynamical systems of natural origination, the question of the nature of chaos remains open so far.

The following speculation indicates possible direction for the study of this question. Note that if a system has an attractor which is structurally stable, then according to conventional hypothesis (the structural stability theorem [23,24]), the attractor is hyperbolic: either trivial (i.e., a stable periodic orbit) or nontrivial. As we mentioned, no one has ever seen nontrivial hyperbolic attractors in natural applications. It follows that if any attractor could be made structurally stable by a small perturbation of the system, then in principle, the study of chaotic dynamics in real systems would be reduced to the study of stable periodic regimes, but this would be quite strange.

An alternative is to try to find nontrivial attractors for systems which lie in the open regions of structural instability in the space of dynamical systems. At the present time two types of such regions are known. The regions of the first type are filled by the systems with Lorenz (quasihyperbolic) attractors. The second are the so-called Newhouse regions with the study of which the present paper deals.

The scope of this paper is to represent recent results of the authors which show that quasi-attractors of systems in the Newhouse regions may exhibit rather nontrivial features which are in a sharp distinction with that one could expect in analogy with stochastic attractors. Thus, we show that the quasistochastic attractors may contain structurally unstable and, moreover, infinitely degenerate periodic orbits are what makes the complete description of dynamics and bifurcations of such attractors impossible in any finite-parameter family.

We also establish that the quasistochastic attractors, in contrast with hyperbolic ones, may not possess the property of self-similarity. Namely, there may exist infinitely many time scales on

[1] Even if these properties may hold, they are not preserved under small perturbations.

which behavior of the system is qualitatively different. Besides, we show that the quasiattractors may simultaneously contain saddle periodic orbits with different topological indices or, what is the same, with different numbers of positive Lyapunov exponents. The last is also impossible for hyperbolic attractors.

Different quasistochastic attractors possess rather different properties (such as "the form" of attractor, the form of power spectrum, fractal dimension, etc.) Nevertheless, it seems to us that the most important property common for them is the presence of *structurally unstable Poincaré homoclinic orbit* either in the system itself or in a nearby system.

Recall that a Poincaré homoclinic orbit is an orbit of intersection of the stable and unstable manifolds of a saddle periodic orbit. A homoclinic orbit is called *structurally stable* if the intersection is transverse, and it is called *structurally unstable* (or *a homoclinic tangency*) if the invariant manifolds are tangent along it (Figure 1).

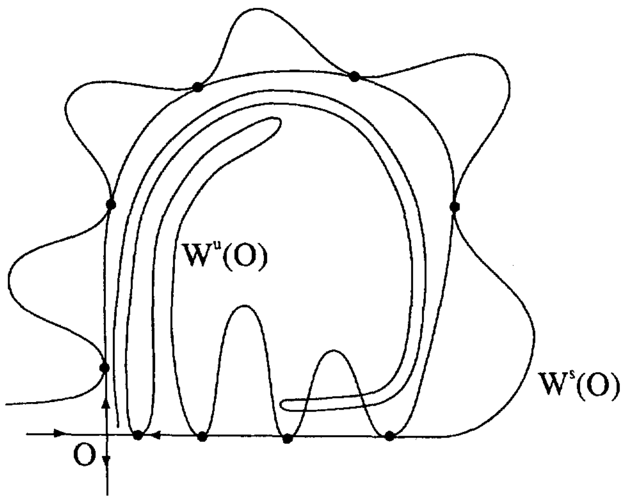

Figure 1. The saddle fixed point O whose the stable W^s and the unstable W^u manifolds have a quadratic tangency at the points of a homoclinic orbit Γ (bold points in the figure).

As it is well known [25,26], in any neighborhood of a structurally stable Poincaré homoclinic orbit there exist nontrivial hyperbolic sets containing a countable number of saddle periodic orbits, continuum of nonperiodic Poisson stable orbits, etc. Thus, the presence of a structurally stable Poincaré homoclinic orbit can be considered as the universal criterium of complex dynamics.

Bifurcations of systems with homoclinic tangencies were studied in a series of papers beginning with [27,28]. An important result was established by Newhouse [29], that in the space of dynamical systems there exist regions (*Newhouse regions*) where systems with structurally unstable Poincaré homoclinic orbits are dense. Moreover, as it was found in [29–31], Newhouse regions exist in any neighbourhood of any system with homoclinic tangency. Namely, the following result is valid.

THEOREM 1. *Let f_ε be a general[2] finite parameter family of dynamical systems which has a saddle periodic orbit L_ε. Suppose that at $\varepsilon = 0$ there exists a structurally unstable homoclinic orbit Γ of the orbit L_0. Then, values of ε for which L_ε has an orbit of quadratic homoclinic tangency are dense in some open regions Δ_i of the parameter space, accumulating at $\varepsilon = 0$.*

The one-parameter version of this theorem was established by Newhouse in [29], for the case of two-dimensional diffeomorphisms and it was extended onto the general multidimensional case by us in [30] (the case with an arbitrary number of parameters follows immediately from [29,30]). The

[2]The exact conditions of general position have been formulated in [30]. In particular, it is required of f_0 that for the tangency to be quadratic, the orbit Γ_0 not lie in the strong stable and strong unstable submanifolds W^{ss} and W^{uu}, etc.

multidimensional case was also considered partly in [31]. This theorem shows that although any given homoclinic tangency can be removed by a small perturbation of the system, the presence of homoclinic tangencies is, nevertheless, a persistent phenomenon.

In our opinion, the presence of structurally unstable Poincaré homoclinic orbits either in the system itself or in a nearby system is one of the main peculiarities of quasistochastic systems. As we can judge, the presence of homoclinic tangencies for some values of parameters was either theoretically proved or found by computer simulations in all dynamical models with quasiattractors (see the list above) for which the problem of finding such parameter values was explicitly set. By Theorem 1, the closure of these parameter values contains open regions. Note that the size of these regions may be rather large in concrete examples (see, for instance, [14]), though the theoretical estimates for the size of the regions Δ_i that can be extracted from the known proof of Theorem 1 give us extremely small values.

We will call as *the Newhouse regions*, such regions in the space of dynamical systems (or in the parameter space while speaking on a finite-parameter family) where systems with homoclinic tangencies are dense. In the case where bifurcations of some system having a saddle periodic orbit with a homoclinic tangency are considered, we reserve the term "Newhouse regions" specifically for those in a small neighborhood of the initial system, where systems are dense which have homoclinic tangencies of the given periodic orbit.

As we see, the problem of studying dynamical phenomena in the Newhouse regions is an important part of the global problem of studying the nature of chaos in real dynamics models. Besides, this problem is of its own interest from the point of view of the qualitative theory and the theory of bifurcations of dynamical systems.

In the present paper, we describe dynamical phenomena in the Newhouse regions for both the two-dimensional and the multidimensional cases. In Sections 2 and 3, we discuss main results (Theorems 2–10). In Section 4, we collect geometrical constructions which determine dynamics near homoclinic tangencies. We restrict ourself by the case of diffeomorphisms: the case of flows can be similarly considered by means of the Poincaré map.

2. MAIN RESULTS: THE TWO-DIMENSIONAL CASE

Before studying the general multidimensional case, we consider the case of two-dimensional maps. Let f be a two-dimensional diffeomorphism having a saddle fixed point O with multipliers λ and γ, where $|\lambda| < 1$, $|\gamma| > 1$. Let W^s and W^u be, respectively, the stable and unstable manifolds of O. Suppose they have a quadratic tangency at the points of some homoclinic orbit Γ (Figure 1).

According to the traditional approach going back to Andronov, to study the bifurcations of a given system is to embed it in an appropriate finite-parameter family, then to divide the parameter space into the regions of structural stability, to determine the bifurcation set, and to split the bifurcation set into connected components corresponding to identical phase portraits (in the sense of topological equivalence). Accordingly, a good model must possess a sufficient number of parameters allowing one to analyze bifurcations of each periodic, homoclinic, heteroclinic orbit occurred.

In a general finite-parameter family containing f, the splitting parameter μ must clearly be one of the main parameters. We define the splitting parameter as follows. Take a point of homoclinic tangency on W^s (the point M^+ in Figures 2 and 3). The manifold W^u has a parabola-like shape near this point for all maps close to f. We denote as μ the distance between W^s and the bottom of the parabola. The sign of μ is chosen such that f_μ has no homoclinic orbits at $\mu > 0$ which are close to Γ, and there are two structurally stable such orbits at $\mu < 0$ (Figure 2).

As we noticed, values of μ for which the map f_μ has "secondary" homoclinic tangencies accumulates at $\mu = 0$. Indeed, take a pair of points belonging to Γ and lying near O : $M^+ \in W^s_{\rm loc}$ and $M^- \in W^u_{\rm loc}$ (see Figure 3). Take μ a bit smaller than zero. Take a piece C of the part of the unstable manifold that lies near M^+ and begin to iterate it. After some number of iterations (the

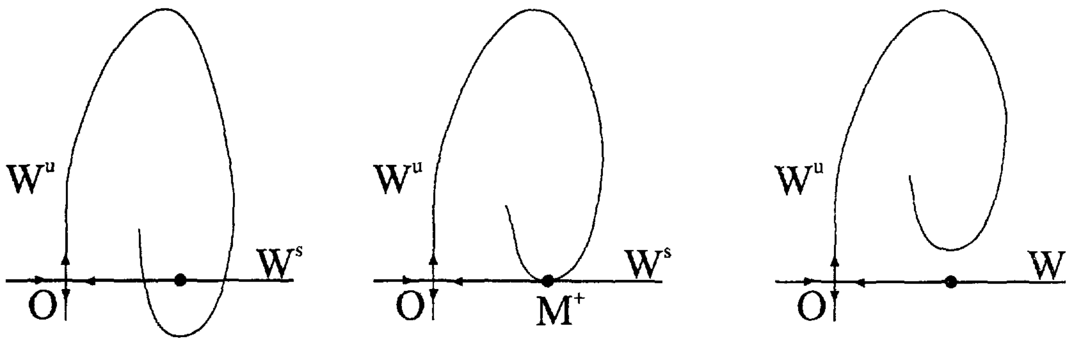

(a) $\mu < 0$. (b) $\mu = 0$. (c) $\mu > 0$.

Figure 2. The splitting parameter μ is chosen such that W^u has a tangency with W^s at a homoclinic point M^+ at $\mu = 0$, there is no homoclinic intersection near M^+ at $\mu > 0$ and there are two points of intersection at $\mu < 0$.

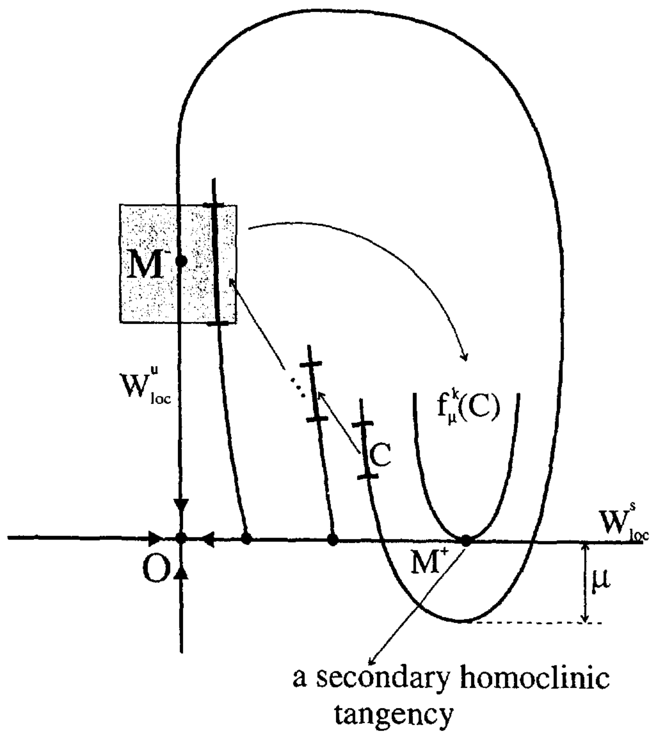

Figure 3. The figure shows how a secondary homoclinic tangency of the manifolds W^s and W^u may be obtained. Take a pair of points which belong to Γ and lie near O : $M^+ \in W^s_{\text{loc}}$ and $M^- \in W^u_{\text{loc}}$. Take μ a bit smaller than zero. Take a piece C of the part of W^u that lies near M^+ and begin to iterate it. After some number of iterations (the closer C is to W^s_{loc}, the larger the number), it may approach a small neighborhood of M^-. Since, at $\mu = 0$, the point M^- goes at M^+ by some finite degree of f, it follows that a small neighborhood of M^- is mapped into a small neighborhood of M^+ by the same degree of f_μ at all small μ. Thus, completing one round along the initial orbit of homoclinic tangency, the curve C may return to a neighborhood of M^+. While doing that, the curve C is expanded and folded, thereby forming a "parabola" $f^k_\mu(C)$ which may clearly have a tangency with W^s_{loc} at some point near M^+, if μ and C are appropriately chosen.

closer C is to the stable manifold, the larger the number), it may approach a small neighborhood of M^-. Since, at $\mu = 0$, the point M^- goes at M^+ by some finite degree of f, it follows that a small neighborhood of M^- is mapped into a small neighborhood of M^+ by the same degree of f_μ at all small μ. Thus, the curve C may return to a neighborhood of M^+ for some number k of iterations of f_μ (we will speak that C makes a single round along Γ). While doing that, the

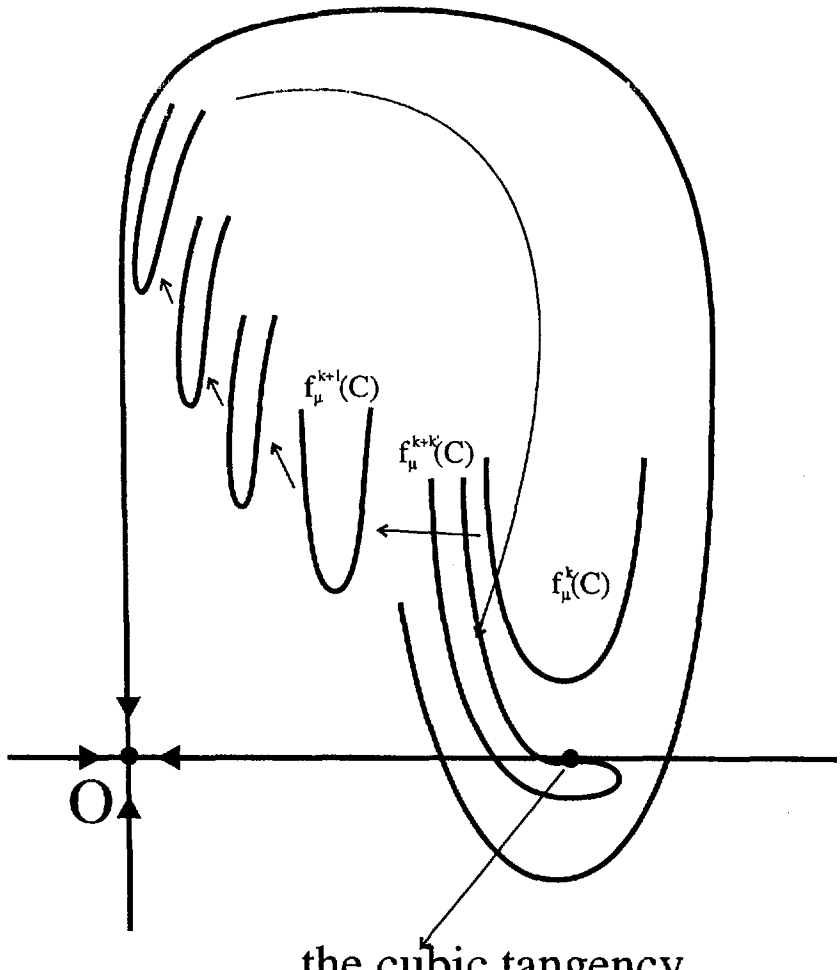

Figure 4. Take μ a bit greater than in Figure 2. Then, after one more round along the initial homoclinic orbit, the image of C takes a distorted form which allows one to obtain a cubic tangency of W^s and W^u.

curve C is expanded and folded, thereby forming "parabola" $f_\mu^k(C)$. Fitting μ and C, one can clearly obtain a secondary homoclinic tangency.

Making more rounds, other homoclinic tangencies can be obtained with an appropriate variation of μ. According to Theorem 1, values of μ corresponding to the multi-round homoclinic tangencies fill densely intervals accumulating at $\mu = 0$.

We note also, that a small perturbation of f may imply cubic homoclinic tangencies. Figure 4 shows how it can be achieved. Consider a system with the secondary homoclinic tangency (Figure 3). We take the parabola $f_\mu^k(C)$ and change μ a little bit, so that the parabola lies above W^s. By some number k' of iterations, the parabola carries out one more round along Γ. The curve $f_\mu^{k+k'}(C)$ is a "distorted parabola" (Figure 4) which can be made cubically tangent to W^s by a small perturbation (for this, two control parameters are necessary).

Increasing the number of rounds along Γ, homoclinic tangencies of higher and higher orders can be obtained in a neighborhood of the initial quadratic tangency. Since systems with quadratic tangencies are dense in the Newhouse regions, we arrive at the following result.

THEOREM 2. *(See [32,33].) Systems with homoclinic tangencies of any order (definite or indefinite) are dense in the Newhouse regions.*

Recall the definition of the order of tangency of two C^r-smooth curves γ_1 and γ_2 on a plane. Let the curve γ_1 be given by the equation $y = 0$ and γ_2 be given by the equation $y = \varphi(x)$,

$\varphi(0) = 0$, in some C^r-coordinates (x, y). If $\frac{\partial^i \varphi}{\partial x^i}(0) = 0$ at $i = 1, \dots, s$ and $\frac{\partial^{s+1} \varphi}{\partial x^{s+1}}(0) \neq 0$ for some $s < r$, then γ_1 and γ_2 have *a tangency of order s* (a quadratic tangency if $s = 1$, a cubic tangency if $s = 2$). In case $\frac{\partial^i \varphi}{\partial x^i}(0) = 0$ at $i = 1, \dots, r$, the curves γ_1 and γ_2 have a tangency of *indefinite* order.

If W^s and W^u have a tangency of order s, then at small perturbations, the equation of W^u in a neighborhood of the point of tangency may be well known and written in the form

$$y = \varepsilon_0 + \varepsilon_1 x + \cdots + \varepsilon_{s-1} x^{s-1} + x^{s+1} + o(x^{s+1}). \tag{2.1}$$

The values ε_i are parameters which control the bifurcations of the intersections of W^u and W^s (the last has the form $y = 0$). We see that the bifurcation analysis requires at least an s-parameter family in this case.

According to Theorem 2, one can obtain tangencies of arbitrarily high order by a small perturbation of the initial map f with the orbit of homoclinic tangency of order 1. Therefore, we have to conclude that no finite number of control parameters is sufficient for the *complete* study of the bifurcations in a small neighborhood of a homoclinic tangency, independently of the order of it.

The impossibility of giving the complete description of the bifurcations of systems with structurally unstable Poincaré homoclinic orbits appears also as the presence of systems with arbitrarily degenerate periodic orbits in the Newhouse regions.

It is well known that if, for some C^r-smooth map, an orbit of period j has one multiplier equal to $\nu = \pm 1$ and all the other multipliers do not lie on the unit circle, then in the case $\nu = 1$, the restriction of the j^{th} degree of the map onto the center manifold can be written either in the form

$$\bar{y} = y + L_s y^{s+1} + o\left(y^{s+1}\right), \qquad 1 \leq s \leq r - 1, \tag{2.2}$$

where the coefficient L_s that is not equal to zero is called s^{th} *Lyapunov value*, or in the form

$$\bar{y} = y + o\left(y^r\right). \tag{2.3}$$

In the case $\nu = -1$, the restriction of the $2j^{\text{th}}$ degree of the map onto the center manifold can be written either in the form

$$\bar{y} = y + L_s y^{2s+1} + o\left(y^{2s+1}\right), \qquad 3 \leq 2s + 1 \leq r, \quad L_s \neq 0, \tag{2.4}$$

or, again in form (2.3). If one of formulas (2.2) or (2.4) holds ($L_s \neq 0$), we speak that the periodic orbit has *the degeneracy of order s*, and in case formula (2.3) holds, we speak about *degeneracy of indefinite or infinite order.*

THEOREM 3. *(See [32,33].) Systems with periodic orbits of any prescribed order (definite or indefinite) of degeneracy are dense in the Newhouse regions (both for the case $\nu = 1$ and for the case $\nu = -1$).*

This theorem is a corollary of Theorem 2. The main element of the proof is the construction of the first return map near a structurally unstable homoclinic orbit of an s^{th} order of tangency (Figure 5). We begin with the initial case of quadratic tangency ($s = 1$). Take a small strip σ in a neighborhood of the point M^+. If the strip is chosen appropriately, it rounds once along Γ and returns in the neighborhood of M^+ for some number k of iterations of f_μ; the image $f_\mu^k(\sigma)$ has the horseshoe shape. We denote the restriction of the map f_μ^k onto σ as T_k and call it *the first return map.* The strip σ is small. Therefore, we rescale coordinates, as in [34], so that it obtains a finite size. In such rescaled coordinates, the map T_k is written in the following form (see Lemma 1 in Section 4):

$$\begin{aligned} \bar{x} &= y + O\left(|\lambda\gamma|^k + |\gamma|^{-k}\right), \\ \bar{y} &= M - y^2 + O\left(|\lambda\gamma|^k + |\gamma|^{-k}\right), \end{aligned} \tag{2.5}$$

where $M \sim \mu\gamma^{2k}$.

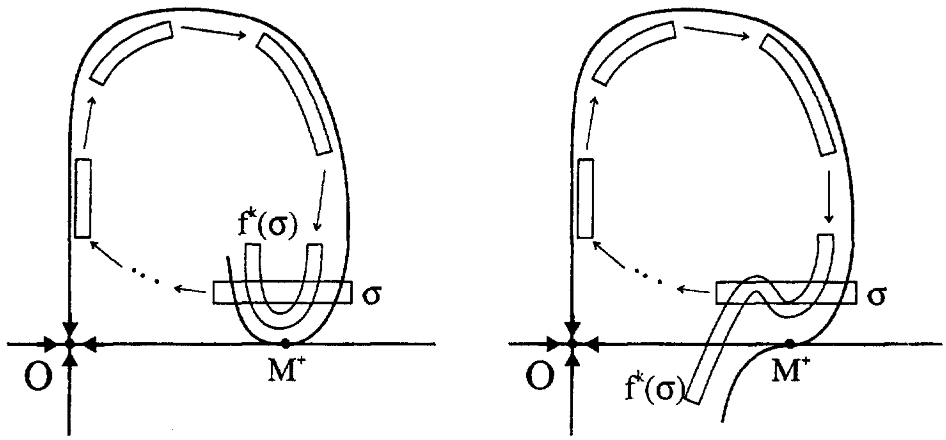

(a) $s = 1$. (b) $s = 2$.

Figure 5. The first return map for the cases of: (a) quadratic tangency; (b) cubic tangency.

Let $|\lambda\gamma| < 1$ (the case $|\lambda\gamma| > 1$ is reduced to the case $|\lambda\gamma| < 1$ by transition from f to its inverse map). Then map (2.5) is close to the well-known one-dimensional parabola map

$$\bar{y} = M - y^2, \tag{2.6}$$

for k large enough; the rescaled splitting parameter M may be take arbitrary finite values (the larger k, the larger the interval of allowed values of M).

In the case of s^{th} order tangency, the rescaled map T_k is close to the one-dimensional map (see Lemma 2 in Section 4)

$$\bar{y} = E_0 + E_1 y + \cdots + E_{s-1} y^{s-1} + y^{s+1} + o\left(y^{s+1}\right), \tag{2.7}$$

where $E_0, E_1, \ldots, E_{s-1}$ are rescaled parameters $\varepsilon_0, \varepsilon_1, \ldots, \varepsilon_{s-1}$ from (2.1) and they may take arbitrary finite values. Particularly, if $E_0 = E_2 = \cdots = E_{s-1} = 0$, $E_1 = \pm 1$, then map (2.7) has a fixed point with the multiplier ± 1 and with the order of degeneracy which can be made arbitrarily high by increasing the value of s. Since T_k is close to map (2.7) it also has a highly degenerate fixed point for $E_0, E_2, \ldots, E_{s-1}$ close to zero and E_1 close to ± 1.

Thus, by a small perturbation of a system with a homoclinic tangency of a large order, one can achieve a periodic orbit of a high order of degeneracy to arise. Since systems with homoclinic tangencies of any order are dense in the Newhouse regions (Theorem 2), it follows that systems with arbitrarily degenerate periodic orbits are also dense there.

We see again that no finite number of control parameters is sufficient for the complete study of the Newhouse regions: now, for the study of the bifurcations of periodic orbits. In other words, from the point of view of the approach traditional to the bifurcation theory, any dynamical model (a finite-parameter family of dynamical systems) is, in terms of [32,33], bad in the Newhouse regions. Apparently, here it is necessary to give up the ideology of complete description and to restrict oneself to the calculation of some average quantities and to the study of certain general properties.

In particular, such a general property is that in the Newhouse regions there exist nontrivial hyperbolic sets; i.e., there is always a countable number of saddle periodic orbits and structurally stable Poincaré homoclinic orbits.

Another important feature of systems in the Newhouse regions is the absence of complete self-similarity. Notice that the homoclinic orbits of high orders of tangency that we obtained by perturbations of the map f make quite a large number of rounds along Γ (for instance, the cubic tangency can be formed after three rounds). It is clear that the higher the order of tangency, the more rounds is required to get it. Near the homoclinic tangencies of high orders there appear the maps described by formula (2.7). Since the first return map near such a tangency corresponds, at the same time, to many rounds along the initial homoclinic orbit Γ, maps close to the map f exhibit dynamics which is described on large time scales by maps (2.7): the larger the number of rounds, the larger the value of s. The maps given by formula (2.7) are completely different for different values of s. Thus, systems belonging to the Newhouse regions may show completely different qualitative behavior on different time scales. Note that nothing similar happens in hyperbolic systems where the number of essential scales is always finite.

One more important feature is the coexistence of orbits of different topological types. If we consider a structurally stable Poincaré homoclinic orbit, then we see that all periodic orbits lying in a small neighborhood of it have a saddle-type [25,26]. On the contrary, near a structurally unstable homoclinic orbit there may well known exist both structurally unstable and attractive periodic orbits in addition to saddle ones. Namely, the following theorem is valid.

THEOREM 4. *(See [27,28].) Let the product of the multipliers of O be less than unity in absolute value: $|\lambda\gamma| < 1$. Then for a general one-parameter family f_μ there exists a sequence of intervals δ_i accumulating at $\mu = 0$, such that at $\mu \in \delta_i$ the map f_μ possesses an attractive periodic orbit in a small neighborhood of Γ and, at μ belonging to the boundary of δ_i, the map has a structurally unstable periodic orbit.*

If $|\lambda\gamma| > 1$, then the analogous result is also valid: the map has here a repelling periodic orbit (a source) for $\mu \in \delta_i$. Theorems 4 and 1 imply the following result.

THEOREM 5. *If $|\lambda\gamma| < 1$, then, for a general one-parameter family f_μ, in the Newhouse regions Δ_i, parameter values are dense for which the map, in addition to a countable number of saddle periodic orbits, also possesses a countable number of attractive[3] periodic orbits.*

In its initial weaker formulation (not for intervals in one-parameter families but for regions in the space of dynamical systems) this theorem was proved in [35]. The proof of the one-parameter version can be obtained, for instance, in the following way. Let $|\lambda\gamma| < 1$ and $\mu_0 \in \Delta_i$. By Theorem 1, arbitrarily close to μ_0 there exists $\mu_1 \in \Delta_i$ such that O has a quadratic homoclinic tangency at $\mu = \mu_1$. By Theorem 4, near $\mu = \mu_1$ there exists a small interval $d_1 \subset \Delta_i$ such that f_μ has an attractive periodic orbit at $\mu \in d_1$. Again, since $d_1 \subset \Delta_i$ there exists a value $\mu_2 \in d_1$ such that O has a quadratic tangency at $\mu = \mu_2$ and some new interval $d_2 \subset d_1$ such that f_μ has one more attractive periodic orbit at $\mu \in d_2$. Repeating the arguments, we obtain, in arbitrary closeness of the given value μ_0, the system of embedded intervals $d_1 \supset d_2 \supset \cdots$ such that f_μ has at least j attractive periodic orbits at $\mu \in d_j$. The intersection of all d_j is nonempty. It contains at least one point μ^* and the map f_μ has a countable number of attractive periodic orbits at $\mu = \mu^*$.

Theorems 4 and 5 provide a theoretical basis for the fact that most presently known strange attractors contain attractive periodic orbits within. As a rule, the attractive periodic orbits in a quasiattractor have very long periods and narrow basins of attraction, and they are hard to observe in applied problems because of the presence of noise. However, in the space of the parameters of the model there can exist regions where individual, relatively short-period attractive periodic orbits can be seen; these regions are called *windows of stability*.

3. MAIN RESULTS: THE MULTIDIMENSIONAL CASE

Theorems 2 and 3 can be extended onto the general multidimensional case [36]. Thus, the conclusion on impossibility of a finite-parameter complete description is also valid for this case. However, the situation connected with the coexistence of periodic orbits of different topological types is considerably more complicated. Here, the windows of stability may contain narrow

[3]Repelling if $|\lambda\gamma| > 1$.

invariant tori and even chaotic attractors. Moreover, not only saddle and attractive (or saddle and repelling) periodic orbits may exist simultaneously, but saddle periodic orbits with the different numbers of positive Lyapunov exponents may also coexist. These statements are based on the results represented below.

Let f be a multidimensional diffeomorphism with a structurally unstable homoclinic orbit Γ of some saddle fixed point O. We are interested in the structure of the set N of all orbits which lie entirely in a small neighborhood U of the set $O \cup \Gamma$.

Suppose the map satisfies some conditions of general position [36] (the tangency is quadratic, Γ does not lie in W^{ss} and W^{uu}, etc.). Let $\lambda_1, \dots, \lambda_m, \gamma_1, \dots, \gamma_n$ be the multipliers of O, $|\gamma_n| \geq \dots \geq |\gamma_1| > 1 > |\lambda_1| \geq \dots \geq |\lambda_m|$. We use the notation $\lambda = |\lambda_1|$, $\gamma = |\gamma_1|$. The multipliers λ_i, γ_j nearest to the unit circle (i.e., those for which $|\lambda_i| = \lambda$, $|\gamma_j| = \gamma$) we call *leading* and the rest we call *nonleading*. The coordinates in a neighborhood of O that correspond to the characteristic directions of these multipliers we call, respectively, leading and nonleading.

We assume that the leading multipliers are simple. We designate the number of leading stable multipliers by p_s and the number of leading unstable multipliers by p_u. Accordingly, we assign the type (p_s, p_u) to the system. The four following cases are possible here:

(1,1). λ_1 and γ_1 are real and $\lambda > |\lambda_2|$, $\gamma < |\gamma_2|$,
(2,1). $\lambda_1 = \bar{\lambda}_2 = \lambda e^{i\varphi}$, γ_1 is real and $\lambda > |\lambda_3|$, $\gamma < |\gamma_2|$,
(1,2). λ_1 is real, $\gamma_2 = \bar{\gamma}_2 = \gamma e^{i\psi}$, and $\lambda > |\lambda_2|$, $\gamma < |\gamma_3|$,
(2,2). $\lambda_1 = \bar{\lambda}_2 = \lambda e^{i\varphi}$, $\gamma_1 = \bar{\gamma}_2 = \gamma e^{i\psi}$, and $\lambda > |\lambda_3|$, $\gamma < |\gamma_3|$.

The following reduction theorem shows that orbit behavior of the map f and all nearby maps is determined, first of all, by dynamics in the leading coordinates.

THEOREM 6. *(See [36].) Under general conditions, for all systems close to f there exists an invariant $(p_s + p_u)$-dimensional C^1-manifold $\mathcal{M}^c$ possessing the following properties.*

1. *The set N of all orbits that lie entirely in U is contained in $\mathcal{M}^c$.*
2. *$\mathcal{M}^c$ is tangent to the leading directions at the point O.*
3. *Along the stable and unstable nonleading directions there are exponential contraction and, respectively, expansion which are stronger that those along directions tangential to $\mathcal{M}^c$.*

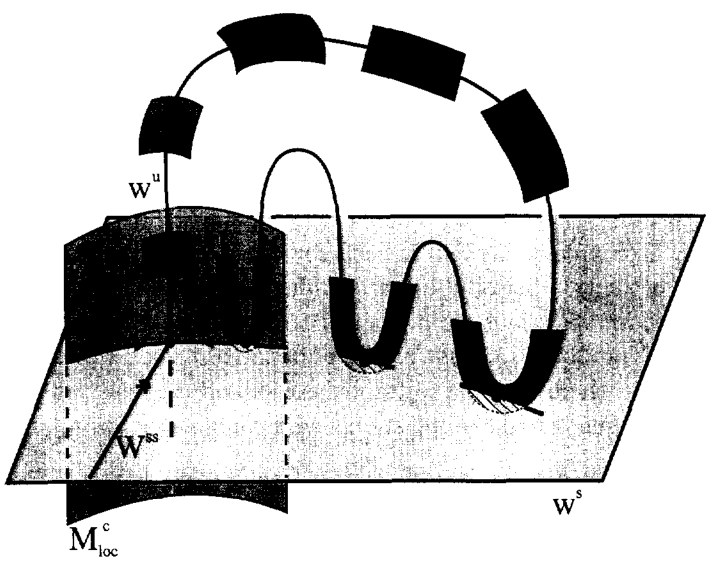

Figure 6. An example of the "center" manifold $\mathcal{M}^c$ (the union of $\mathcal{M}^c_{\text{loc}}$ with the dashed regions outside $\mathcal{M}^c_{\text{loc}}$ in the figure) for the three-dimensional case where the multipliers λ_2, λ_1, and γ of the fixed point are such that $0 < \lambda_2 < \lambda_1 < 1 < \gamma$.

Figure 6 represents an example of the manifold $\mathcal{M}^c$ for the three-dimensional case where the multipliers of O are such that $0 < \lambda_2 < \lambda_1 < 1 < \gamma_1$. In the terms that we have introduced,

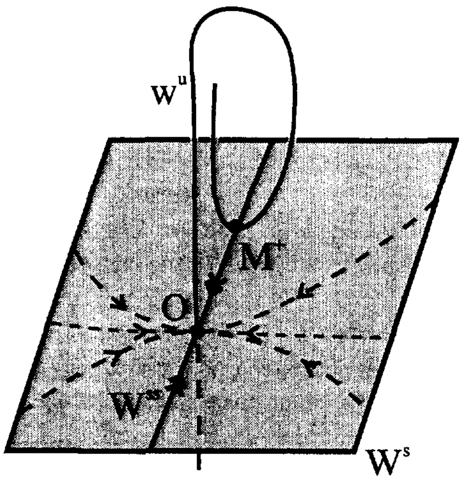

(a) The orbit of tangency belongs to W^{ss}.

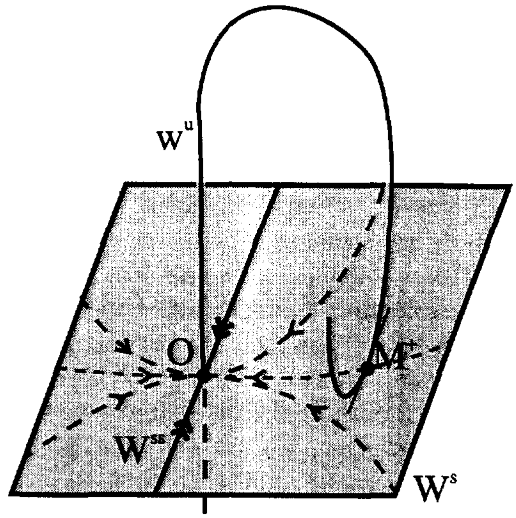

(b) The vector that is tangent to W^s and W^u at M^+ is parallel to the nonleading eigendirection.

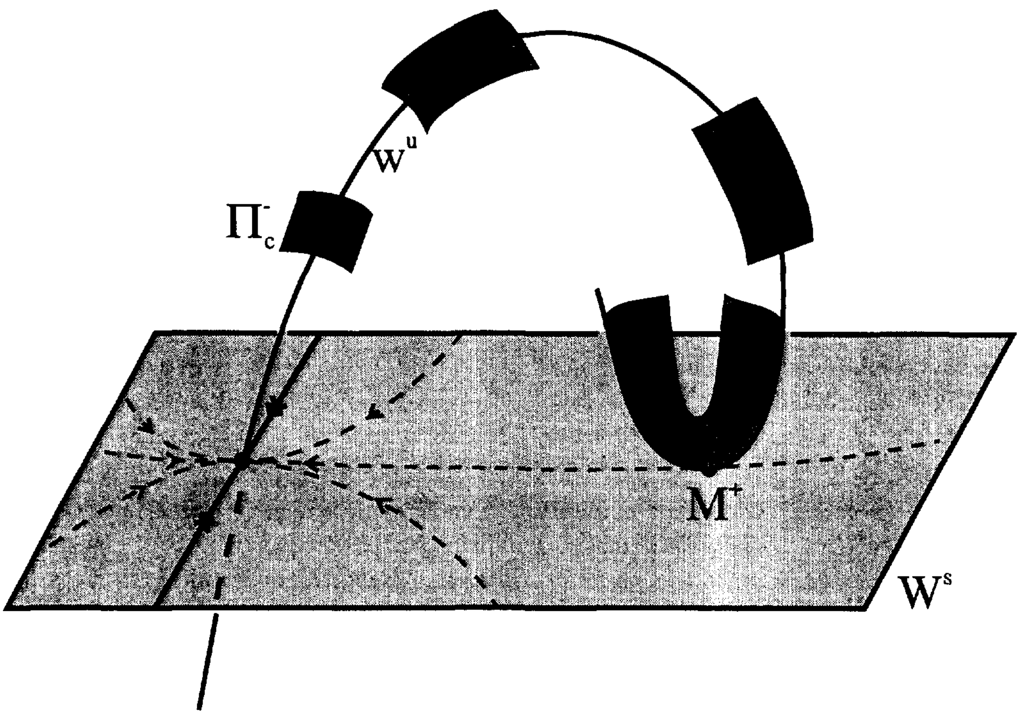

(c) The image of the surface Π_c^- is tangent to W^s at W^+.

Figure 7. The exceptional cases where the smooth invariant manifold does not exist.

this is Case (1,1) where λ_1 and γ_1 are the leading multipliers and λ_2 is the nonleading stable multiplier. The point O is the fixed point of the stable node-type for the restriction of the map f onto W^s. The nonleading manifold W^{ss} exists in W^s such that iterations of any point of W^{ss} tend to O like a geometric progression with the ratio λ_2. The orbits lying in $W^s \setminus W^{ss}$ tend to O along the leading eigendirection and the distance to O decreases as a geometric progression with the ratio λ_1.

In this case, in a small neighborhood of O there are well known [37] to exist two-dimensional invariant C^1-manifolds each of which contains W^u_{loc} and intersects W^s at a curve tangential to the leading direction. According to Theorem 6, at least one of them, $\mathcal{M}^c_{\rm loc}$, can be extended along the orbits of f, forming a global attractive invariant manifold $\mathcal{M}^c$ which contains Γ. The manifold $\mathcal{M}^c$ is attractive in the sense, any point that do not belong to $\mathcal{M}^c$ leave the small neighborhood U of Γ with the iterations of the inverse map f^{-1}. This implies that $\mathcal{M}^c$ contains the whole set N of orbits lying in U entirely. The invariance of $\mathcal{M}^c$ means that if one takes a small area $\Pi_c^- \subset \mathcal{M}^c_{\rm loc}$ containing the point M^- of Γ and iterates this area k times, then it returns in the neighborhood of O for some k, so that $f^k(\Pi_c^-) \subset \mathcal{M}^c_{\rm loc}$ (Figure 6).

This occurs possible if the map f satisfy some conditions of general position. The excluded cases where the smooth invariant manifold does not exist are shown in Figure 7: the homoclinic orbit Γ belongs to W^{ss} (Figure 7a); the vector tangential to W^u at M^+ is parallel to the nonleading eigenvector (Figure 7b); the surface $f^k(\Pi_c^-)$ is tangent to W^s at M^+ (Figure 7c).

The reduction theorem immediately give us essential restrictions on possible types of orbits of the set N for the map f itself and for all nearby maps. Thus, since there is a strong exponential contraction along the stable nonleading directions and the number of such linearly independent directions is $(m - p_s)$, orbits of N must have at least $(m - p_s)$ negative Lyapunov exponents. Analogously, the strong expansions along the nonleading unstable directions causes that orbits of N must have at least $(n - p_u)$ positive Lyapunov exponents. This means that dimensions of stable and unstable manifolds of any periodic orbit in U may not be less than $(m - p_s)$ and $(n - p_u)$, respectively. In particular, if O has unstable nonleading multipliers (i.e., $p_u < n$), then neither f nor any nearby map has attractive periodic orbits in U.

In general, these restrictions are not final. More precise estimates for the number of positive and negative Lyapunov exponents can be found if one consider the $(p_s + p_u)$-dimensional map which is the restriction of the initial map onto $\mathcal{M}^c$.

Let us introduce the quantity D which is equal to the absolute value of the product of all leading multipliers, i.e., $D = \lambda^{p_s}\gamma^{p_u}$. Note that D is the Jacobian of the restriction of f onto $\mathcal{M}^c$, calculated at the point O. If $D < 1$, then the map $f|_{\mathcal{M}^c}$ contracts $(p_s + p_u)$-dimensional volumes exponentially near O, and if $D > 1$, then it expands the volumes. Since any orbit that lies in U, entirely spends most of the time in a small neighborhood of O, the map $f|_{\mathcal{M}^c}$ contracts $(p_s + p_u)$-dimensional volumes in a neighborhood of the orbit at $D < 1$ and it expands the volumes at $D > 1$. Therefore, any orbit of N has at least one negative Lyapunov exponent at $D < 1$ and it has at least one positive Lyapunov exponent at $D > 1$.

If to summarize what is said above, we arrive at the following result.

THEOREM 7. *(See [36].) Let f be a map with a homoclinic tangency in general position. If the saddle fixed point O has unstable nonleading multipliers ($p_u < n$) or if $D > 1$, then neither f nor maps close to it have attractive periodic orbits in a small neighborhood of $O \cap \Gamma$.*

A statement that is, in a sense, opposite to this theorem, is also valid.

THEOREM 8. *(See [36].) If O has no unstable nonleading multipliers ($p_u = n$) and if $D < 1$, then systems with infinitely many attractive periodic orbits are dense in the Newhouse regions Δ_i.*

This theorem does not follow from the reduction theorem. Here, the proof is based on the study of the first return map T_k of some small strip σ close enough to M^+. Note that the maps T_k may be different in different situations. Namely, let O, do not have unstable nonleading multipliers and let $D < 1$. Then, in the case $(p_s, p_u) = (1,1)$, the map T_k is close to the one-dimensional map (like in the two-dimensional case; see the previous section)

$$\bar{y} = M - y^2, \tag{3.1}$$

in some rescaled coordinates. The same formula holds in the case $(p_s, p_u) = (2,1)$ at $\lambda\gamma < 1$. In both cases, only one variable is relevant and all the others are suppressed by strong contraction.

In the case $(p_s, p_u) = (2,1)$ at $\lambda\gamma > 1$, the rescaled map T_k is close to the Hénon map

$$\bar{x} = y, \qquad \bar{y} = M - y^2 - Bx, \tag{3.2}$$

at an appropriate choice of σ.

In the cases $(p_s, p_u) = (1, 2)$ and $(p_s, p_u) = (2, 2)$ at $\lambda\gamma^2 < 1$, the rescaled map T_k is close, for the appropriately chosen σ, to the map

$$\bar{x} = y, \qquad \bar{y} = M - x^2 - Cy, \tag{3.3}$$

and, in the case $(p_s, p_u) = (2, 2)$ at $\lambda\gamma^2 > 1$, it is close to the map

$$\bar{x} = y, \qquad \bar{y} = z, \qquad \bar{y} = M - y^2 - Cz - Bx, \tag{3.4}$$

where M is the rescaled splitting parameter μ, and B and C are some trigonometric functions of $k\varphi$ and $k\psi$, respectively. At k large enough, parameters M, B, and C may take arbitrary finite values.

The last two maps have not been studied sufficiently, unlike the parabola map (3.1) and the Hénon map (3.2). However, the bifurcation analysis of the fixed points of these maps is comparatively simple. Thus, for each of maps (3.1)–(3.4) one can easily find parameter values such that there exists an attractive fixed point.

Thus, an analogue of Theorem 4 is valid: *if there are no unstable nonleading multipliers and if $D < 1$, then a small perturbation of f can provide an appearance of an attractive periodic orbit*. Unlike to the two-dimensional case, in dependence on the situation, not only the splitting parameter μ may be required here, but also there may be necessary the perturbation of values φ and ψ which control the variation of B and C, respectively.

By the use of the construction with the system of embedded disks (analogous to that applied in the two-dimensional case at the proof of Theorem 5), the theorem on infinitely many attractive periodic orbits (Theorem 8) follows immediately now for the Newhouse regions Δ_i in corresponding one-, two-, or three-parameter families.

Actually, the analysis of fixed points of maps (3.1)–(3.4) allows us to establish much more than the existence of attractive periodic orbits. Thus, for maps (3.2) and (3.3) there exist the values of M and, respectively, B or C at which the map has a fixed point with a pair of multipliers equal to unity in absolute value, while map (3.4) has a fixed point with three multipliers equal to unity in absolute value for some M, B, and C. If we select now the three cases (recall that $D = \lambda^{p_s}\gamma^{p_u}$ is less than one):

(1^+) $(p_s, p_u) = (1, 1)$, or $(p_s, p_u) = (2, 1)$ and $\lambda\gamma < 1$,
(2^+) $(p_s, p_u) = (2, 1)$ and $\lambda\gamma > 1$, or $(p_s, p_u) = (1, 2)$ or $(p_s, p_u) = (2, 2)$ and $\lambda\gamma^2 < 1$,
(3^+) $(p_s, p_u) = (2, 2)$ and $\lambda\gamma^2 > 1$,

then we arrive at the following result.

THEOREM 9. *(See [36].) Suppose that $D < 1$. Then, in Case (1^+), systems having periodic orbits with l multipliers equal to unity in absolute value are dense in the Newhouse regions Δ_i.*

This theorem has quite nontrivial consequences. Note that an invariant curve can be born from the points with two unit multipliers (an invariant torus, if we consider a flow) and chaotic attractors can be formed in the case of three multipliers equal to unity in absolute value. For instance, an attractor similar to the Lorenz attractor can be born at local bifurcations of a fixed point with two multipliers equal to -1 and one equal $+1$, and a spiral attractor can be born in the case of three multipliers equal to -1 (see [38,39], where an analysis of corresponding normal forms is carried out).

Using the construction with embedded disks again, we find that *systems with infinitely many invariant tori and systems with infinitely many coexisting chaotic attractors are dense in the Newhouse regions in Cases (2^+) and (3^+), respectively.*

To conclude, we consider the question on the coexistence of saddle periodic orbits with different numbers of positive Lyapunov exponents.

THEOREM 10. *(See [36].) Let $D < 1$, and let O have no unstable nonleading multipliers.*[4] *Then, in Case* (1^+), *systems that for any $j = 0, \dots, l$ have a countable number of periodic orbits with j multipliers greater than unity in absolute value are dense in the Newhouse regions Δ_i. At the same time, no map close to f can have, in a small neighborhood U of $O \cup \Gamma$, a periodic orbit with more than l multipliers greater than unity in absolute value.*

The second part of the theorem follows from the easily verified fact that, in Case (1^+), the map f (and any nearby map) contracts exponentially $(l+1)$-dimensional volumes on $\mathcal{M}^c$ in a small neighborhood of O, and hence, in a small neighborhood of any orbit lying in U entirely. Therefore, any such orbit cannot have more than l positive Lyapunov exponents.

The first part of the theorem is proved by the linear analysis or fixed points of maps (3.1)–(3.4): for any of these maps, regions of parameter values can be easily found where the map has a fixed point with j multipliers greater than unity in absolute value ($0 \le j \le l$). This implies that, for any $j = 0, \dots, l$, a periodic orbit with j positive Lyapunov exponents can arise at an arbitrarily small perturbation of f in a corresponding l-parameter family. Using the construction with embedded disks again, we find that the parameter values are dense in the Newhouse regions Δ_i at which the map has now infinitely many such orbits simultaneously for each $j = 0, \dots, l$.

Theorem 10 has a direct relation to the problem of *hyperchaos*. Usually, those attractors are called hyperchaotic for which more than one positive Lyapunov exponent is found. As we see, in contrast with hyperbolic systems, the number of positive Lyapunov exponents may vary for different orbits if the system belongs to a Newhouse region. It is not clear, therefore, in what sense the number of positive Lyapunov exponents can be considered as a characteristics of the system as a whole. At the same time, considerations based on estimates of contraction and expansion of volumes are still effective here: the quantity l in Theorem 10 is none other than the integral part of the Lyapunov dimension calculated at the point O by the Kaplan-Yorke formula [40] for the restriction of the map f onto the "center" (or "inertial") manifold $\mathcal{M}^c$.

4. GEOMETRIC CONSTRUCTIONS AND CALCULATIONS

We discuss here in greater detail, the geometric constructions that determine the dynamics near homoclinic tangencies. First, we consider the two-dimensional case. Namely, we consider a C^r-smooth ($r \ge 3$) two-dimensional diffeomorphism f, which has a saddle fixed point O with multipliers λ and γ where $0 < |\lambda| < 1$, $|\gamma| > 1$. We consider the case where $|\lambda\gamma| < 1$. Suppose the stable and unstable manifolds of O have a quadratic tangency at the points of the homoclinic orbit Γ.

Let U be a small neighborhood of the set $O \cup \Gamma$. The neighborhood U is the union of a small disc U_0 containing O, and of a finite number of small disks surrounding the points of Γ which are located outside U_0 (Figure 8). We denote by N the set of orbits of the map f that lie entirely in U. Let T_0 be the restriction of f onto U_0 (it is called *the local map*). Note that the map T_0 in some C^{r-1}-coordinates (x, y) can be written in the form [41,42]

$$\bar{x} = \lambda x + f(x,y)x^2 y, \qquad \bar{y} = \gamma y + g(x,y)xy^2. \tag{4.1}$$

By (4.1), the equations of the local stable manifold W^s_{loc} and local unstable manifold W^u_{loc} are $y = 0$ and $x = 0$, respectively. The representation (4.1) is convenient in that, in these coordinates the map T_0^k for any sufficiently large k is linear in the lowest order. Specifically, we have the following representation [41] of the map $T_0^k : (x_0, y_0) \mapsto (x_k, y_k)$

$$\begin{aligned} x_k &= \lambda^k x_0 + |\lambda|^k |\gamma|^{-k} \xi_k(x_0, y_k), \\ y_0 &= \gamma^{-k} y_k + |\gamma|^{-2k} \eta_k(x_0, y_k), \end{aligned} \tag{4.2}$$

[4]The contribution of the unstable nonleading multipliers is trivial: instead of "j multipliers greater than unity" we should write "$(n - p_u + j)$ multipliers ...;" the case $D > 1$ is reduced to the case $D < 1$ by considering the map f^{-1} instead of f, so everywhere through the theorem the words "greater than unity" should be replaced by "less than" in this case.

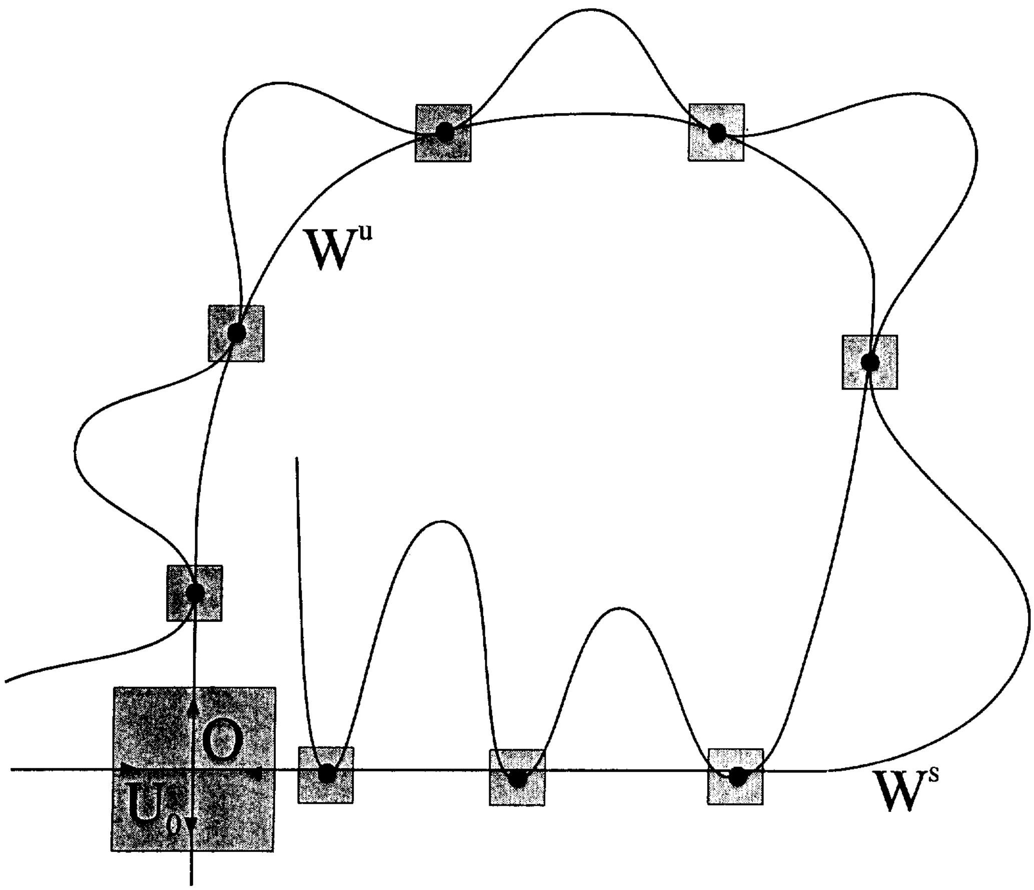

Figure 8. The neighborhood U of the contour $O \cup \Gamma$ (bold points in the figure) is a union of a small disk U_0 containing O and of a finite number of small neighborhoods of that points of Γ which lie outside U_0.

where ξ_k and η_k are functions uniformly bounded at all k along with their derivatives up to the order $(r-2)$.

Let $M^+(x^+,0)$ and $M^-(0,y^-)$ be a pair of points of Γ which lie in U_0 and belong to W^s_{loc} and W^u_{loc}, respectively. Without loss of generality, we can assume $x^+ > 0$ and $y^- > 0$. Let Π^+ and Π^- be sufficiently small neighborhoods of the homoclinic points M^+ and M^- such that $T_0(\Pi^+) \cap \Pi^+ = \emptyset$ and $T_0(\Pi^-) \cap \Pi^- = \emptyset$. Evidently, there exists an integer q such that $f^q(M^-) = M^+$. We denote the map $f^q : \Pi^- \to \Pi^+$ as T_1 (it is called *the global map*, see Figure 9). The map T_1 can obviously be written in the form

$$
\begin{aligned}
\bar{x} - x^+ &= ax + b(y - y^-) + \cdots , \\
\bar{y} &= cx + d(y - y^-)^2 + \cdots ,
\end{aligned} \tag{4.3}
$$

where $bc \neq 0$ since T_1 is a diffeomorphism, and $d \neq 0$ since the tangency is quadratic.

Note that the orbits of N must intersect the neighborhoods Π^+ and Π^- (otherwise, these orbits would be far from Γ). However, not all orbits that start in Π^+ arrive in Π^-. The set of the points whose orbits get into Π^- form a countable number of strips $\sigma^0_k = \Pi^+ \cap T_0^{-k}\Pi^-$ that accumulate on W^s. The way of constructing these strips is obvious from Figure 10. In turn, the images of the strips σ^0_k under the maps T_0^k give on Π^- a sequence of vertical strips σ^1_k that accumulate on W^u_{loc} (Figure 11).

The images of the strips σ^1_k under the map T_1 have the shape of horseshoes, accumulating on the "parabola" $T_1 W^u_{\text{loc}}$ (Figure 13). It is clear that the orbits of N must intersect Π^+ at the points of intersection of the horseshoes $T_1\sigma^1_j$ and the strips σ^0_i. Therefore, the structure of the

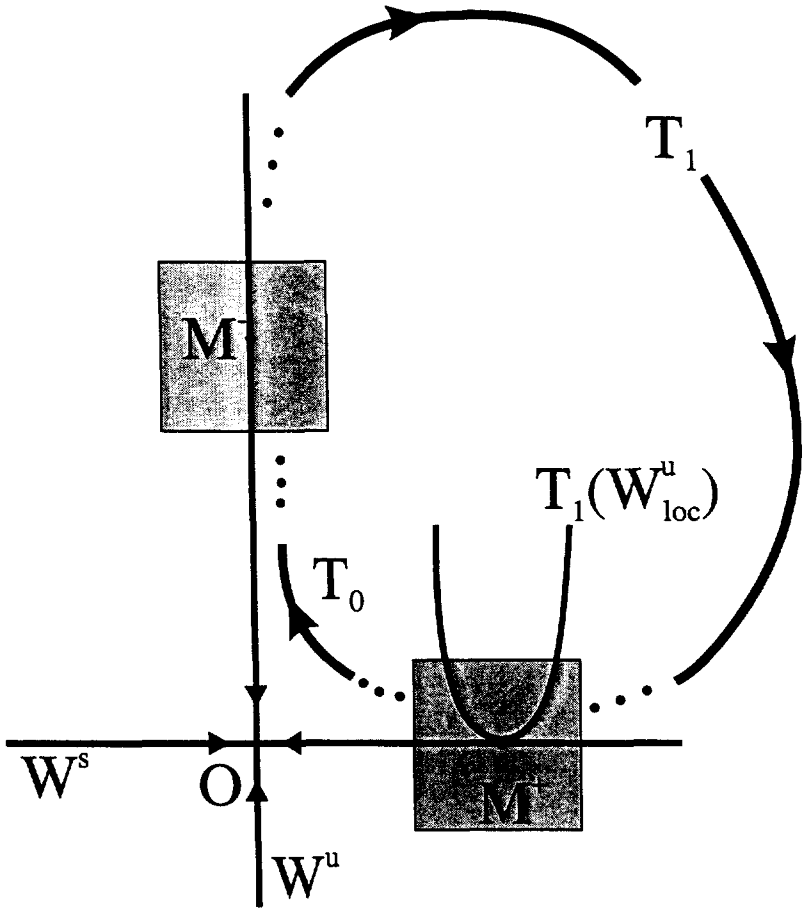

Figure 9. The local and global maps T_0 and T_1.

set N depends strongly on the geometric properties of the intersection of the horseshoes and the strips.

To be specific, we shall assume that $\lambda > 0$ and $\gamma > 0$. Then, depending on the signs of c and d, four different cases of mutual arrangement of the manifolds W^s_{loc} and $T_1 W^u_{\text{loc}}$ are possible [27,28] (Figure 12). If $T_1 W^u_{\text{loc}}$ is tangent to W^s_{loc} from below ($d < 0$) (Figures 12a,b), then the set N has a trivial structure: $N = \{O, \Gamma\}$ [27,28]. This is related to the fact that here the intersection $T_1\sigma^1_i \cap \sigma^0_j$ can be nonempty only for $j > i$, since the strip σ^0_j lies at a distance of the order of γ^{-j} from W^s_{loc}, and the top of the strip $T_1\sigma^1_i$ lies at a distance of the order of $\lambda^i \ll \gamma^{-i}$ from it (Figure 13a). Note that in the case $c < 0$ and $d < 0$ the strips $T_1\sigma^1_i$ and σ^0_j lie on different sides of W^s_{loc} for any i and j, and therefore, $T_1\sigma^1_i \cap \sigma^0_j = \emptyset$ in this case (Figure 13b).

If $T_1 W^u_{\text{loc}}$ is tangent to W^s_{loc} from above ($d > 0$) (Figure 12c,d), then the set N will now contain nontrivial hyperbolic subsets. If $c < 0$ and $d > 0$, then for any i and j the intersection of $T_1\sigma^1_i$ with σ^0_j is regular, i.e., it consists of two connected components (Figure 13c). In this case, the set N can be shown [27,28] to be in one-to-one correspondence with the quotient system of the Bernoulli shift with three-symbols $\{0, 1, 2, \}$ which is obtained by identifying the two homoclinic orbits: $(\dots, 0, \dots, 0, 1, 0, \dots, 0, \dots)$ and $(\dots, 0, \dots, 0, 2, 0, \dots, 0, \dots)$. Hereat, all orbits of $N \setminus \Gamma$ are of the saddle-type.

In the case $c > 0$, $d > 0$, the set N also contains nontrivial hyperbolic subsets [27,28,43] but, in general, these subsets do not exhaust the set N. The reason is that there, besides regular intersections of the horseshoes and the strips, there may also be nonregular intersections (Figure 13d). The existence of attractive and structurally unstable orbits is associated with the latter [44,45].

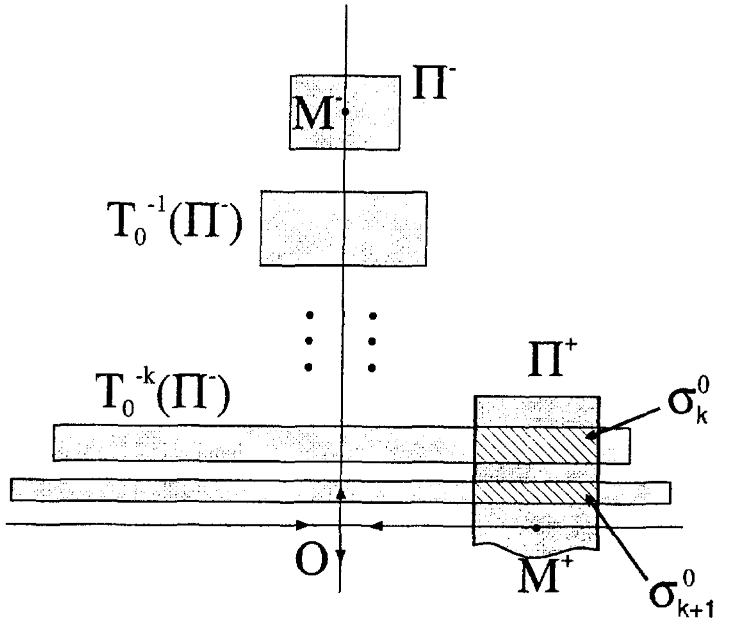

Figure 10. This figure illustrates the construction of the strips σ_k^0, lying on Π^+, such that σ_k^0 is the domain of definition of the map $T_0^k : \Pi^+ \to \Pi^-$. The points on Π^+ that lie in Π^- after k iterations of the map T_0, belong to the set $T_0^{-k}(\Pi^-) \cap \Pi^+$. The neighborhood Π^- is contracted in the vertical direction by a factor of γ^{-1} and expanded in the horizontal direction by a factor of λ^{-1} under the action of the map T_0^{-1}, and moreover, $T_0^{-1}(\Pi^-) \cap \Pi^- = \emptyset$. Correspondingly, the set $T_0^{-k}(\Pi^-)$ in a narrow rectangular are expanded along the x axis and displaced from it by a distance of the order of γ^{-k}. Moreover, the rectangles $T_0^{-k}(\Pi^-)$ and $T_0^{-(k+1)}(\Pi^-)$ do not intersect. For sufficiently large k, the intersection of $T_0^{-(k)}(\Pi^-)$ with Π^+ is a strip σ_k^0 as in the figure. As $k \to \infty$, the strips σ_k^0 accumulate on the segment $W^s \cap \Pi^+$.

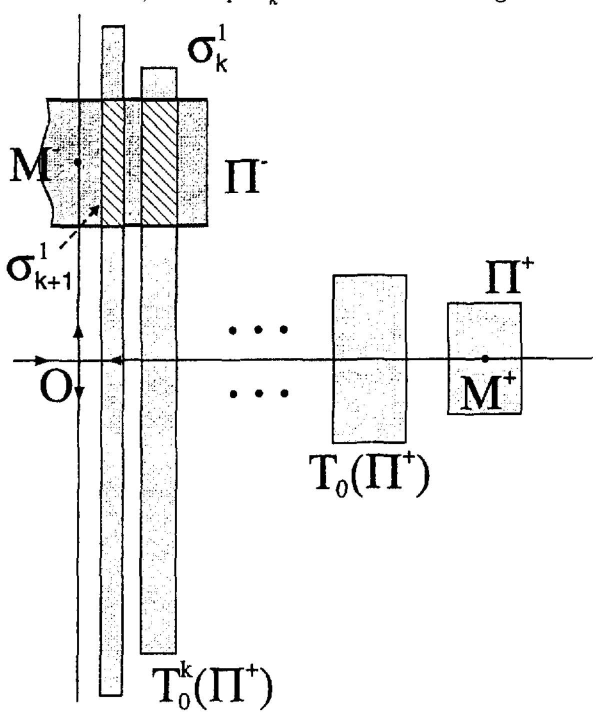

Figure 11. The range of the map $T_0^k : \Pi^+ \to \Pi^-$ is the vertical strip σ_k^1.

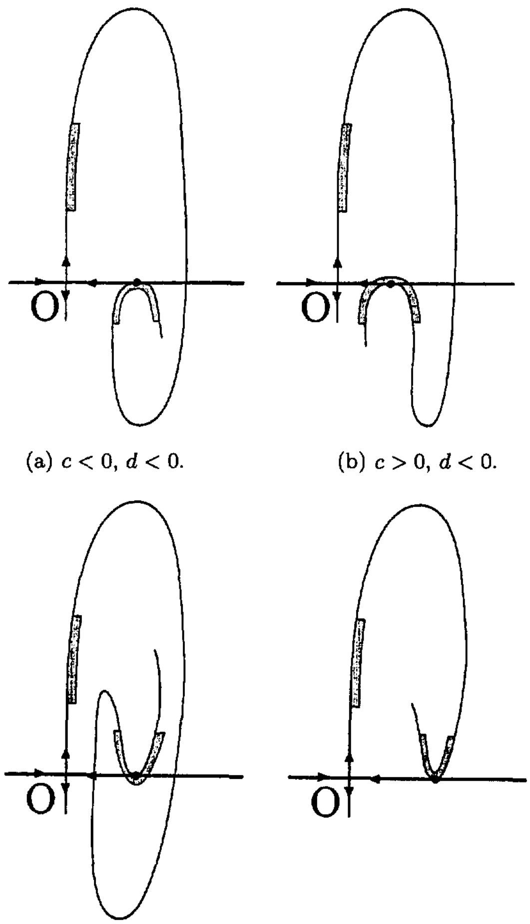

(a) $c < 0$, $d < 0$.　(b) $c > 0$, $d < 0$.

(c) $c < 0$, $d > 0$.　(d) $c > 0$, $d > 0$.

Figure 12. The four different cases of homoclinic tangencies. These cases differ not only in the mutual arrangement of the stable and unstable manifolds (tangent from below: Figures (a) and (b); tangent from above: Figures (c) and (d), but also in that how the shaded semineighborhood of the point M^- is mapped into the neighborhood of the point M^+ under the action of the global map T_1. If $\lambda > 0$ and $\gamma > 0$, these four cases are distinguished by the combinations of signs of the parameters c and d of the map T_1.

Below, to be specific, we consider only the case $c > 0$, $d > 0$. To describe maps close to f we must introduce the splitting parameter μ: when $\mu < 0$, the parabola $T_1 W^u_{\text{loc}}$ intersects W^s_{loc} at two points; when $\mu = 0$, the parabola $T_1 W^s_{\text{loc}}$ is tangent to W^s_{loc} at one point, and when $\mu > 0$ there is no intersection. It is clear that if the bottom of the parabola descends sufficiently low (large and negative μ), then each horseshoe intersects each strip. In this case, the set N_μ is a hyperbolic set similar to the invariant set in the Smale horseshoe. However, if μ is sufficiently large and positive, then the horseshoes and the strips do not intersect at all, and all of the orbits except O will escape from U.

The main question is what happens when the parameter μ varies from the large negative to the large positive values. First of all, it is necessary to study the structure of the bifurcation set corresponding to one strip, that is, to study the bifurcations in the family of the first return maps $T_k(\mu) \equiv T_1 T_0^k : \sigma_k^0 \to \sigma_k^1$. The following result is valid.

LEMMA 1. *The map $T_k(\mu)$ can be brought to the form*

$$\begin{aligned} \bar{x} &= y + O\left(\lambda^k \gamma^k + \gamma^{-k}\right), \\ \bar{y} &= M - y^2 + O\left(\lambda^k \gamma^k + \gamma^{-k}\right), \end{aligned} \tag{4.4}$$

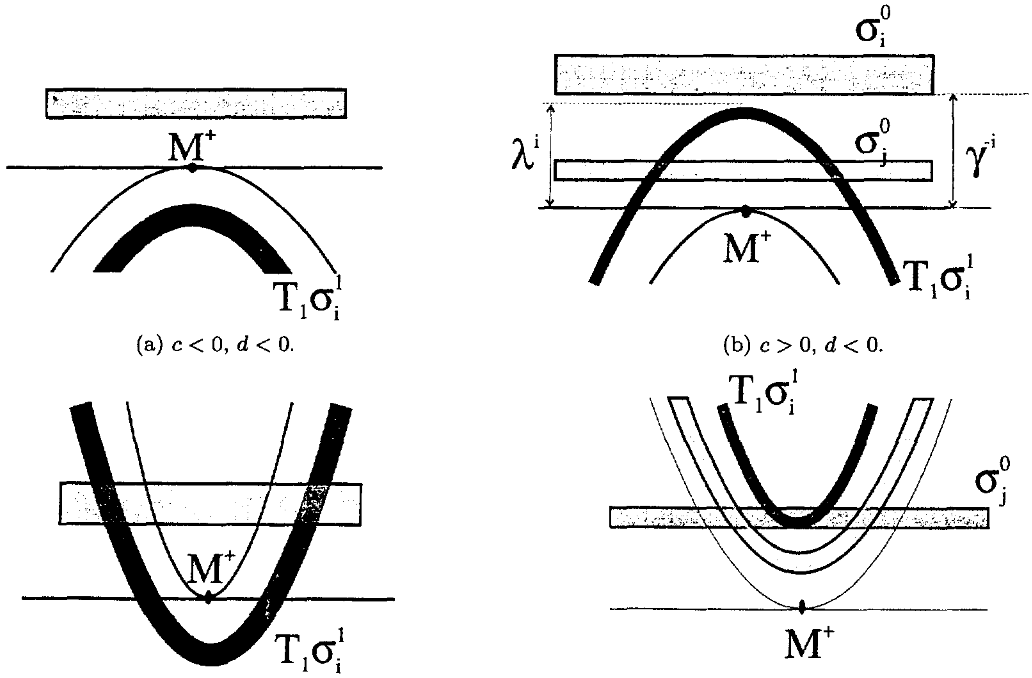

Figure 13. Basic elements of the geometry of the intersection of a strip σ_i^0 and a horseshoe $T_1(\sigma_j^1)$ for the case $|\lambda\gamma| < 1$. In the case of tangency from below (Figures (a) and (b)), the horseshoe $T_1(\sigma_i^1)$ lies below "its" strip σ_i^0. In this case, either $T_1(\sigma_i^1)$ intersects the strips σ_j^0 only if $j \gg i$ (the case $c > 0$, $d < 0$) or it does not intersect any strips at all (the case $c < 0$, $d < 0$). For this reason, the structure of the set N is trivial in this case: $N = O \cup \Gamma$.

In the case of tangency from above (Figures (c) and (d)), the horseshoe $T_1(\sigma_i^1)$ intersects "its" strip (σ_i^0) regularly, thereby forming the geometric configuration of the Smale's horseshoe example. Just from this fact it is possible to infer that the structure of the set N is nontrivial here. The difference in the cases $c < 0$, $d > 0$ and $c > 0$, $d > 0$ is that the intersection of any horseshoe with any strip is regular in the first case, while in the latter case there can be nonregular as well as regular intersections. As a result, all the orbits of the set N except Γ can be shown to be of the saddle-type in the case $c < 0$, $d > 0$, whereas in the case $c > 0$, $d > 0$ there can be structurally unstable and attractive periodic orbits in N (moreover, systems with arbitrarily degenerate periodic and homoclinic orbits are dense in the set of systems with homoclinic tangencies of this type).

by means of a linear transformation of the coordinates and the parameter; here the rescaled splitting parameter $M = -d\gamma^{2k}(\mu - \gamma^{-k}y^- + \cdots)$ may take arbitrary finite values for sufficiently large k.

PROOF. Take a point $(x_0, y_0) \in \sigma_k^0$. Let $(x_k, y_k) = T_0^k(x_0, y_0)$, $(\bar{x}_0, \bar{y}_0) = T_1(x_k, y_k) \equiv T_k(x_0, y_0)$, $(\bar{x}_k, \bar{y}_k) = T_0^k(\bar{x}_0, \bar{y}_0)$. By (4.1),(4.2), the map $T_k(\mu)$ is written in the form

$$\begin{aligned} \bar{x} - x^+ &= a\lambda^k x(1 + \cdots) + b(y - y^-) + \cdots, \\ \gamma^{-k}\bar{y}\left(1 + \gamma^{-k}\eta_k(\bar{x}, \bar{y})\right) &= \mu + c\lambda^k x(1 + \cdots) + d(y - y^-)^2 + \cdots, \end{aligned} \tag{4.5}$$

where we use the notation $x = x_0$, $\bar{x} = \bar{x}_0$, $y = y_k$, $\bar{y} = \bar{y}_k$.

With the shift of the origin: $y \to y + y^-$, $x \to x + x^+$, we write the map $T_k(\mu)$ in the form

$$\begin{aligned} \bar{x} &= by + O\left(\lambda^k\right) + O\left(y^2\right), \\ \gamma^{-k}\bar{y} + \gamma^{-2k}O(\bar{y}) &= M_1 + dy^2 + \lambda^2 O\left(|x| + |y|\right) + O\left(y^3\right), \end{aligned} \tag{4.6}$$

where

$$M_1 = \mu + c\lambda^k x^+ - \gamma^{-k}y^- + \cdots. \tag{4.7}$$

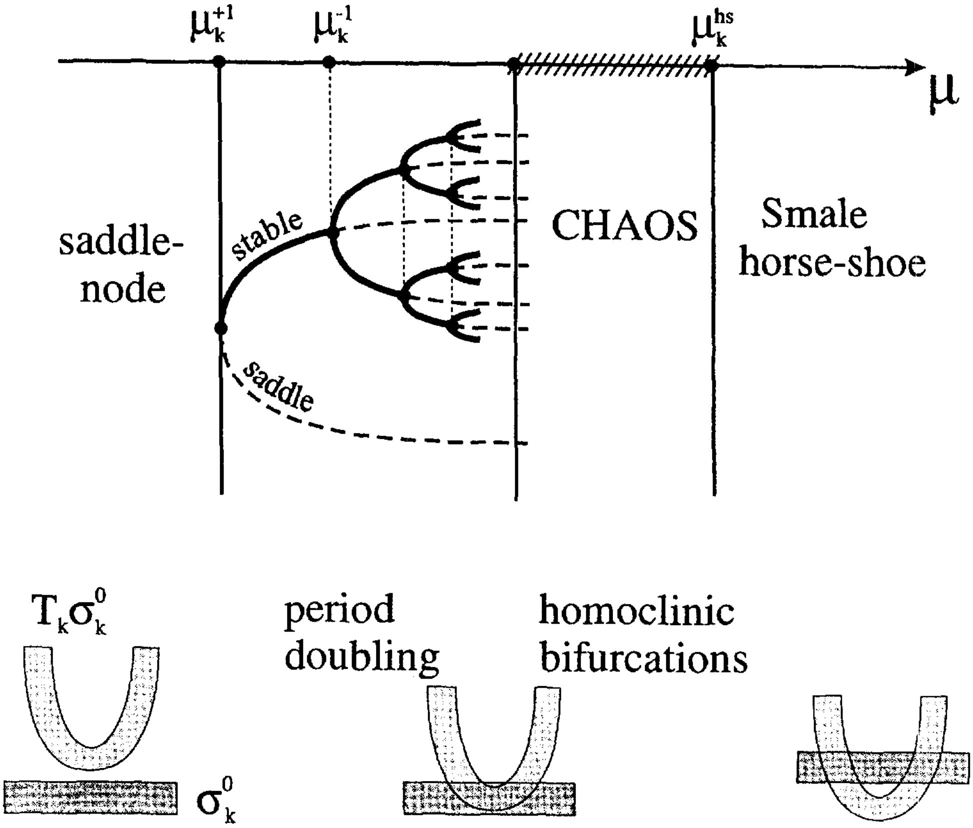

Figure 14. The bifurcation interval $[\mu_k^{+1}, \mu_k^{hs}]$ that corresponds to the sequence of bifurcations in the development of the Smale horseshoe on the strip σ_k^0, beginning with the first bifurcation of the generation of a saddle-node fixed point at $\mu = \mu_k^{+1}$ and ending with the last one corresponding to a homoclinic tangency for $\mu = \mu_k^{hs}$, after which the horseshoe appears.

Now, rescaling the variables:

$$x \to -\frac{b}{d}\gamma^{-k}x, \qquad y \to -\frac{1}{d}\gamma^{-k}y,$$

brings equations (4.6) to form (4.4) where $M = -d\gamma^{2k}M_1$. This completes the proof of the lemma.

Map (4.4) is close to the one-dimensional parabola map

$$\bar{y} = M - y^2, \tag{4.8}$$

whose bifurcations have been well studied, so that it is possible to recover the bifurcation picture for the initial map T_k. For the parabola map, the bifurcation set is contained in the interval $[-(1/4), 2]$ of values of M : at $M = -1/4$ there appears a fixed point with the multiplier equal to $+1$, this fixed point is attractive at $M \in (-(1/4), (3/4))$ and it undergoes a period-doubling bifurcation at $M = 3/4$; the cascade of period-doubling bifurcations lead to chaotic dynamics which alternates with stability windows and the bifurcations stop at $M = 2$, when the restriction of the map onto the nonwandering set becomes conjugate to the Bernoulli shift of two symbols and it no longer bifurcates as M increases.

By Lemma 1, similar bifurcations take place for the map T_k (see Figure 14). The map has an attractive fixed point O_k at $\mu \in (\mu_k^{+1}, \mu_k^{-1})$ which arises at the saddle-node bifurcation at $\mu = \mu_k^{+1}$ and loses stability (at $\mu = \mu_k^{-1}$) at the period-doubling bifurcation. Here

$$\mu_k^{+1} = \gamma^{-k}y^- - c\lambda^k x^+ + \frac{1}{4d}\gamma^{-2k} + \cdots,$$
$$\mu_k^{-1} = \gamma^{-k}y^- - c\lambda^k x^+ - \frac{3}{4d}\gamma^{-2k} + \cdots,$$

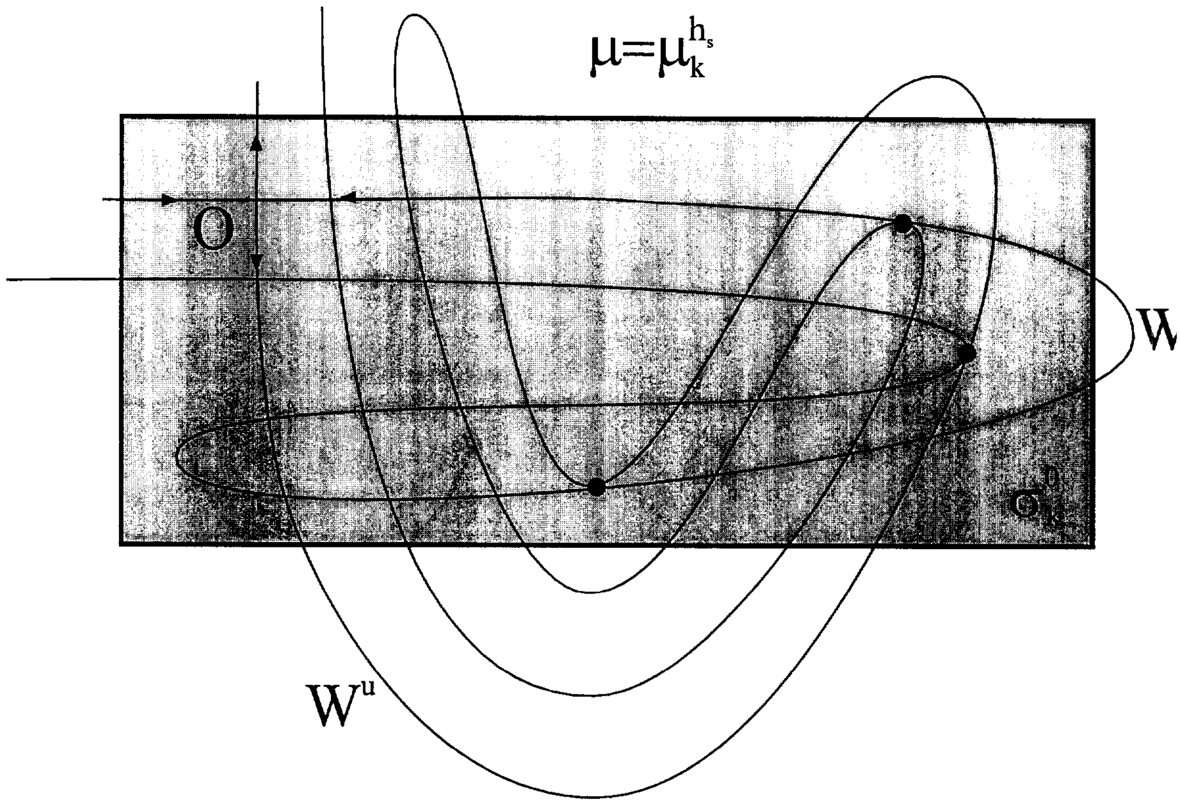

Figure 15. A homoclinic tangency, the last in the sequence of bifurcations in the development of the Smale's horseshow (this is the tangency corresponding to the case shown in the Figure 13c).

Note, that we have found the intervals where the map f_μ possesses the attractive single-round periodic orbit and this is the main element of the proof of Theorem 4 in Section 2.

The bifurcation set of the map T_k is contained in the interval $[\mu_k^{+1}, \mu_k^{hs}]$, where

$$\mu_k^{hs} = \gamma^{-k}y^- - c\lambda^k x^+ - \frac{2}{d}\gamma^{-2k} + \cdots .$$

At $\mu = \mu_k^{hs}$, the fixed point of T_k has the last homoclinic tangency (Figure 15) and an invariant set similar to those of the Smale's horseshoe example arises after this bifurcation. Note, that these bifurcational intervals do not intersect each other for different k.

Clearly, in addition to the orbits that intersect Π^+ each time in the same strip, the map f_μ also has orbits that jump among the strips with various indices. The bifurcation intervals corresponding to these orbits can now overlap. This is the case already for orbits that jump among two strips σ_i^0, σ_j^0 and their images, the horseshoes $T_i\sigma_i^0$ and $T_j\sigma_j^0$. Figure 16 shows the case where there exist completely developed Smale horseshoes on σ_i^0 and σ_j^0 but the upper horseshoe intersects the lower strip in a "nonregular" manner, and new structurally unstable orbits can arise as a result. In particular, using this construction, one can obtain new heteroclinic (Figure 16a) or homoclinic (Figure 16b) tangencies. Moreover, there exist here also periodic orbits "jumping" from one strip to another (they correspond to the fixed points of the double-round return map $T_jT_i : \sigma_i^0 \to \sigma_i^0$). The regions of stability of these double-round periodic orbits can overlap for various i and j, even a countable number of these regions may have common points. In particular, in the set of maps with the homoclinic tangency (in the case $c > 0$, $d > 0$) the maps with a countable number of attractive periodic orbits of this type are dense [44,45].

The geometric construction with two horseshoes was also a basic element of the proof of Theorem 1. Figure 17 shows the bihorseshoe used for the proof. In this situation, the invariant set of

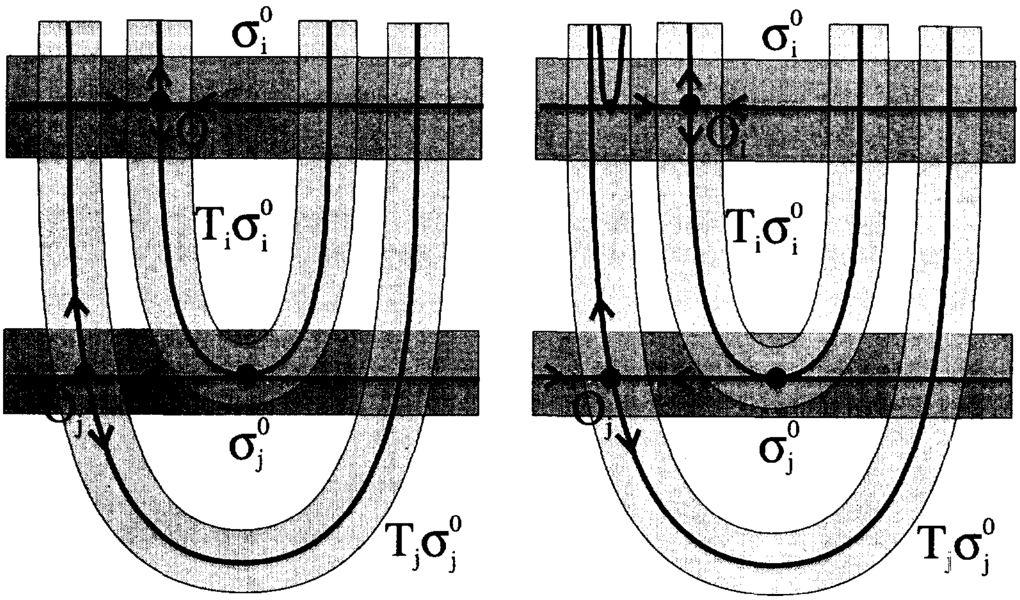

(a) (b)

Figure 16. This figure shows how new heteroclinic or homoclinic tangencies are obtained. Here, on the strips σ_i^0 and σ_j^0 there are already developed Smale's horseshoes for the maps T_i and T_j, respectively, but the upper horseshoe intersects the lower strip "nonregularly." In Figure (a), the manifold $W^u(O_i)$ is tangent to $W^s(O_j)$. In Figure (b), a piece $W^u(O_i) \cap \sigma_j^0$ of the unstable manifold of the point O_i lies just slightly above the stable manifold of the point O_j and the curve $T_j(W^u(O_i) \cap \sigma_j^0)$ which is a part of the manifold $W^u(O_i)$ is tangent to $W^s(O_i)$; i.e., a homoclinic tangency of the invariant manifolds of O_i takes place.

the map T_i on σ_i^0 is a completely developed Smale horseshoe. The map T_j on σ_j^0 is close to the moment of the last tangency; i.e., the value of the parameter μ is close to μ_j^{hs}. At this moment, unstable whiskers of the hyperbolic set that lies in σ_i^0 are tangent, at points of some smooth curve, to stable whiskers of the hyperbolic set that lies in σ_j^0. The latter, in intersection with the curve of tangency, form a specific (thick) Cantor set, what, as Newhouse has shown, is the reason for the nonremovable nature of the tangency.

If we use not two, but a larger number of strips, then we can obtain degenerate homoclinic tangencies and periodic orbits. In particular, when three horseshoes are used, then cubic orbits can be formed. Figure 18 shows three horseshoes where $W^u(O_i)$ and $W^s(O_j)$ are quadratically tangent, as are $W^u(O_j)$ and $W^s(O_k)$. The next figure (Figure 19) illustrates how from one of these structurally unstable contours one can, by a small perturbation, obtain a cubic tangency of the manifolds $W^u(O_i)$ and $W^s(O_k)$.

Taking into account a larger number of strips is a quite complicated problem. We bypass the difficulties if note, instead of calculating the multi-round return map, that due to Theorem 2, homoclinic tangencies of high orders can appear when a piece of W^u makes many rounds along the initial homoclinic orbit Γ. Therefore, the multi-round return maps can presumably be modelled by the first return maps near orbits of highly degenerate tangencies.

These maps are easily calculated. Indeed, let a two-dimensional diffeomorphism f have an orbit of homoclinic tangency of some order s. In this case, the local map T_0 still has the form given by (4.1),(4.2); the global map can be written in the form

$$\begin{aligned} \bar{x} - x^+ &= ax + b(y - y^-) + \cdots, \\ \bar{y} &= cx + d(y - y^-)^{s+1} + \cdots, \end{aligned} \tag{4.9}$$

where, in the first equation, the dots stand for the second (and more) order terms and, in the second equation, for the terms of the order $o(|x| + |y - y^-|^{s+1})$.

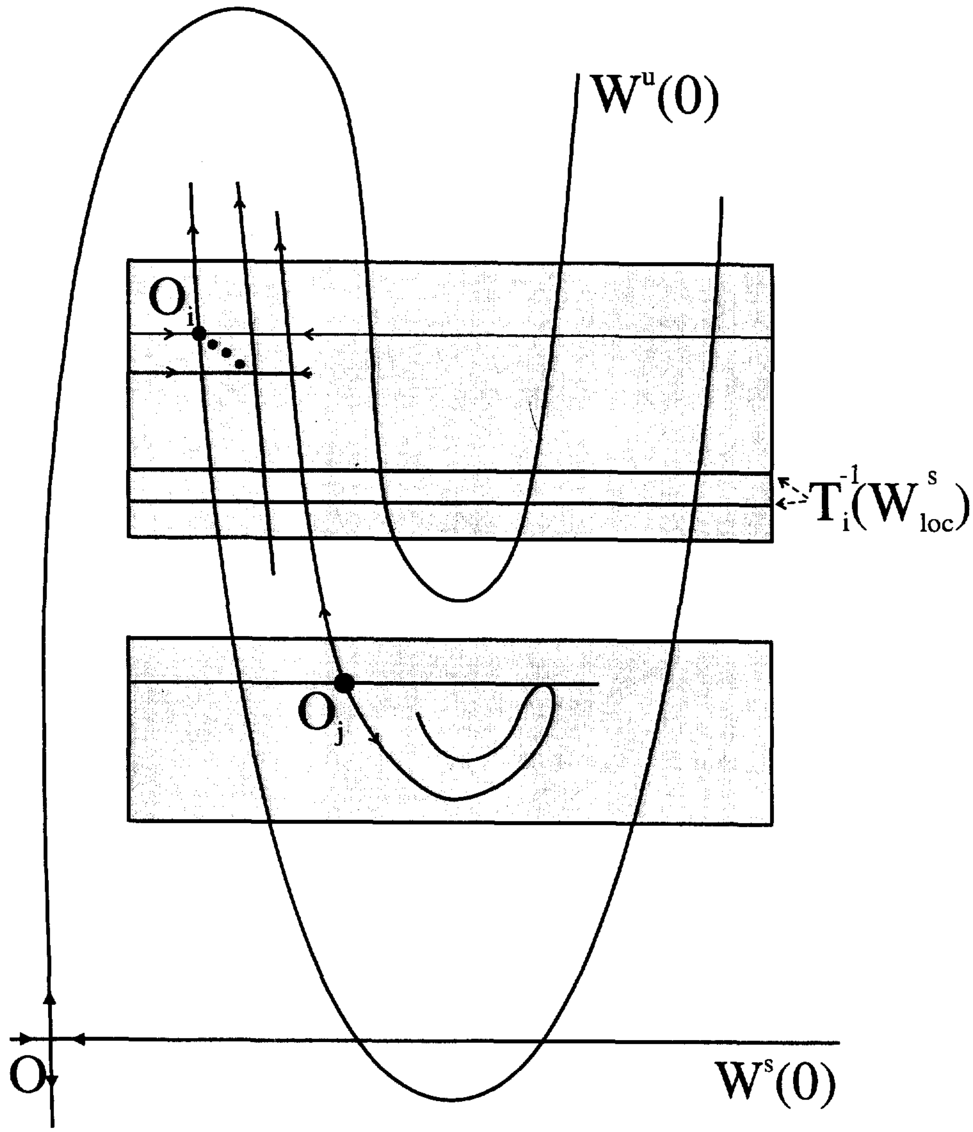

Figure 17. The bihorseshoe used for the proof of Theorem 1. In this situation, the invariant set of the map T_i on σ_i^0 is the developed Smale horseshoe. The map T_j on σ_j^0 is close to the moment of the last tangency; i.e., the value of the parameter μ is close to μ_j^{hs}. At this moment unstable whiskers of the hyperbolic set on σ_i^0 touch the stable whiskers of some hyperbolic subset on σ_j^0.

Consider an s-parameter family f_ε, $\varepsilon = (\varepsilon_0, \ldots, \varepsilon_{s-1})$, of maps close to f ($f_0 \equiv f$) where parameters ε are chosen such that they provides a general unfolding of the given tangency between W^u and W^s (see formula (2.1)). In this case, the global map takes the form

$$\begin{aligned} \bar{x} - x^+ &= ax + b(y - y^-) + \cdots, \\ \bar{y} &= cx + \varepsilon_0 + \varepsilon_1(y - y^-) + \cdots + \varepsilon_{s-1}(y - y^-)^{s-1} + d(y - y^-)^{s+1} + \cdots . \end{aligned} \tag{4.10}$$

Let us now consider the first return map $T_k(\varepsilon)$. The following lemma shows that it is close to a polynomial one-dimensional map.

LEMMA 2. *The map T_k can be brought to the form*

$$\begin{aligned} \bar{x} &= y + O\left(\lambda^k \gamma^k + \gamma^{-k/s}\right), \\ \bar{y} &= E_0 + E_1 y + \cdots + E_{s-1} y^{s-1} + d y^{s+1} + O\left(\lambda^k \gamma^k + \gamma^{-k/s}\right), \end{aligned} \tag{4.11}$$

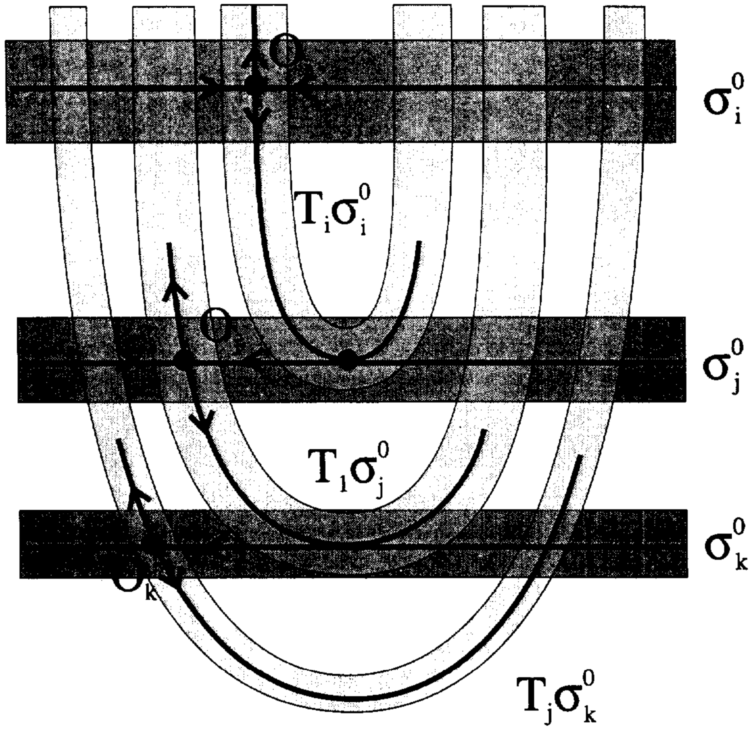

Figure 18. The geometric construction by which it is possible to obtain cubic tangencies. Three horseshoes are shown, where $W^u(O_i)$ and $W^s(O_j)$, as well as $W^u(O_j)$ and $W^s(O_k)$ are tangent.

by a linear transformation of the coordinates and the parameters. Here $E_0 = \gamma^{k(1+1/s)}(\varepsilon_0 - \gamma^{-k}y^- + \cdots)$, $E_i = \gamma^k\gamma^{-k/s(i-1)}\varepsilon_i$.

PROOF. By (4.2),(4.10), the map T_k is written in the following form (see the proof of Lemma 1):

$$\begin{aligned}\bar{x} - x^+ &= a\lambda^k x(1+\cdots) + b(y-y^-) + \cdots,\\ \gamma^{-k}\bar{y}\left(1+\gamma^{-k}\eta_k(\bar{x},\bar{y})\right) &= c\lambda^k x(1+\cdots)\\ &\quad + \varepsilon_0 + \varepsilon_1(y-y^-) + \cdots + \varepsilon_{s-1}(y-y^-)^{s-1} + d(y-y^-)^{s+1} + \cdots.\end{aligned}$$

By the shift of the origin $x \to x + x^+$, $y \to y + y^-$, this map is brought to the form

$$\begin{aligned}\bar{x} &= by + O\left(\lambda^k\right) + O\left(y^2\right),\\ \gamma^{-k}\bar{y} + \gamma^{-2k}O(\bar{y}) &= \left(\varepsilon_0 - \gamma^{-k}y^- + c\lambda^k x^+ + \cdots\right) + \varepsilon_1 y + \cdots + \varepsilon_{s-1}y^{s-1} + dy^{s+1}\\ &\quad + O\left(y^{s+2}\right) + \lambda^k O\left(|x| + |y|\right).\end{aligned}$$

If we rescale the variables and the parameters as follows:

$$\begin{gathered} x \to b\gamma^{-k/s}x, \qquad y \to \gamma^{-k/s}y,\\ \left(\varepsilon_0 - \gamma^{-k}y^- + c\lambda^k x^+ + \cdots\right) \to \gamma^{-k(1+1/s)}E_0,\\ \varepsilon_i \to \gamma^{-k}\gamma^{k/s(i-1)}E_i,\end{gathered}$$

then the map takes form (4.11). The lemma is proved.

Returning to the initial quadratic homoclinic tangency, we see that for large numbers of rounds along the homoclinic orbit, the multi-round return maps are close to arbitrary one-dimensional polynomial maps in some regions of the parameter space and the degree of the polynomials becomes arbitrarily large when the number of rounds increases. Thus, these multi-round maps in a neighborhood of a single homoclinic tangency represent the whole one-dimensional dynamics.

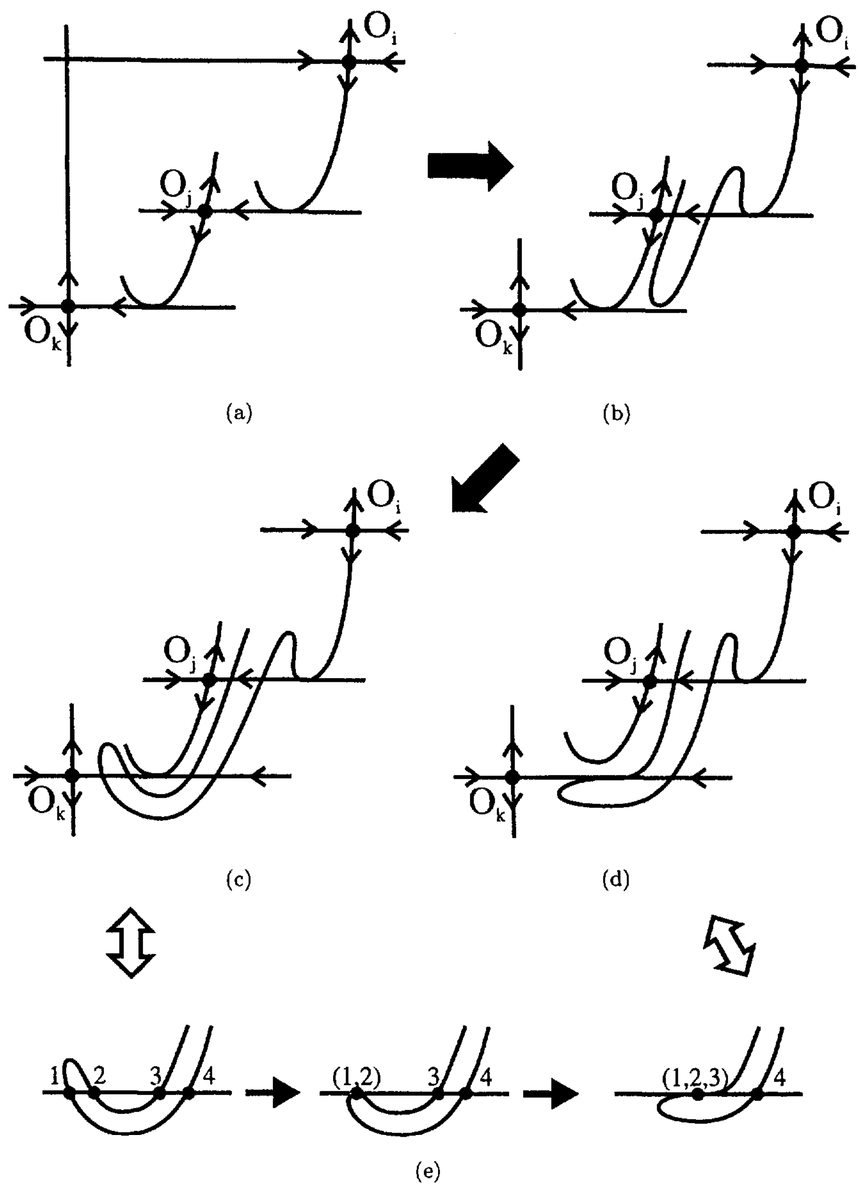

Figure 19. This figure shows how, from a contour with two quadratic heteroclinic tangencies (Figure (a)), one can obtain a cubic tangency (Figure (d)). First, by a small perturbation we make $W^u(O_i)$ intersect $W^s(O_j)$ transversely and make some piece of the manifold $W^u(O_i)$ lie just slightly above $W^s(O_k)$ (Figure (b)). Then we make $W^u(O_i)$ intersect $W^s(O_k)$ in four points (Figure (c)). There is a special path (Figure (e)) from Figure (b) to Figure (c) on which a cubic tangency of the manifolds $W^u(O_i)$ and $W^s(O_k)$ (Figure (d)) takes place.

In conclusion, we look at the structure of the set of strips for the multi-dimensional case. We also show how the procedure of rescaling the first return map works here.

Let f be a multidimensional C^r-diffeomorphism ($r \geq 3$) with a saddle fixed point O whose stable manifold W^s is m-dimensional and the unstable manifold W^u is n-dimensional. Let W^s and W^u have a quadratic tangency at the points of a homoclinic orbit Γ.

A small neighborhood U of $O \cup \Gamma$ is the union of a small $(n+m)$-dimensional disc U_0, and a finite number of small $(n+m)$-dimensional neighborhoods of the points of Γ which lie outside U_0. Like in the two-dimensional case, we denote the restriction $f|_{U_0}$ as T_0. The standard form of the map T_0 corresponds to the coordinates at which the local stable and unstable manifolds of O are straightened: $W^u_{\rm loc} = \{x = 0, u = 0\}$, $W^s_{\rm loc} = \{y = 0, v = 0\}$ in some coordinates (x, y, u, v). This

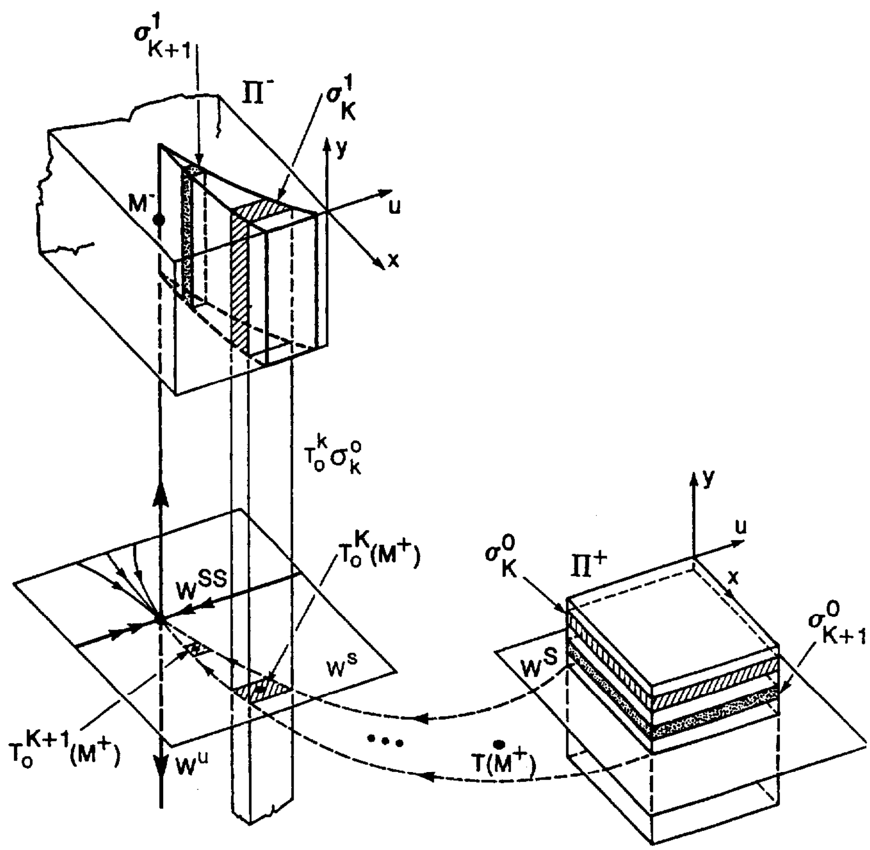

Figure 20. The case of a three-dimensional map where the multipliers λ_1, λ_2, and γ_1 of the fixed point O are such that $0 < \lambda_2 < \lambda_1 < 1 < \gamma_1$. Here the strips $\sigma_k^0 \subset \Pi^+$ are three-dimensional "plates," accumulating on $W^s \cap \Pi^+$ as $k \to \infty$. The strips σ_k^1 lie in a wedge abutting $W^u \cap \Pi^-$, asymptotically contracted along the nonleading coordinate u and tangent to the leading plane $u = 0$ everywhere on $W^u \cap \Pi^-$.

allows one to write T_0 in the form

$$\begin{aligned} \bar{x} &= A_1 x + f_{11}(x,y,v)x + f_{12}(x,y,u,v)u, & \bar{u} &= A_2 u + f_{21}(x,y,v)x + f_{22}(x,y,u,v)u, \\ \bar{y} &= B_1 x + g_{11}(x,u,y)y + g_{12}(x,y,u,v)v, & \bar{v} &= B_2 v + g_{21}(x,u,y)y + g_{22}(x,y,u,v)v, \end{aligned} \tag{4.12}$$

where f_{ij} and g_{ij} vanish at the origin. Here, the eigenvalues of the matrices A_1 and B_1 are the leading multipliers of O, and the eigenvalues of A_2 and B_2 are the nonleading multipliers. Correspondingly, x and y are leading coordinates and u and v are nonleading coordinates. If λ_1 is real, the matrix A_1 has the form $A_1 = (\lambda_1)$, and it has the form $A_1 = \lambda \begin{pmatrix} \cos\varphi & -\sin\varphi \\ \sin\varphi & \cos\varphi \end{pmatrix}$ for complex λ_1. For real γ_1, the matrix B_1 has the form $B_1 = \gamma_1$, and it has the form $B_1 = \gamma \begin{pmatrix} \cos\psi & -\sin\psi \\ \sin\psi & \cos\psi \end{pmatrix}$ if γ_1 is complex.

Like it was done in [2,44], it can be shown that the multidimensional map T_0 reduces to a form that is analogous in a sense to expression (3.4) which we have for the two-dimensional case. Namely, the following identities hold in some C^{r-1}-coordinates:

$$\begin{aligned} f_{i1}|_{x=0} &\equiv 0, & f_{1j}|_{(y=0,v=0)} &= 0, \\ g_{i1}|_{y=0} &\equiv 0, & g_{1j}|_{(x=0,u=0)} &= 0. \end{aligned} \tag{4.13}$$

Analogously to the two-dimensional case, in such coordinates the map T_0^k is linear in the lowest order. Specifically, the map $T_0^k : (x_0, y_0, u_0, v_0) \mapsto (x_k, y_k, u_k, v_k)$ for sufficiently large k can be

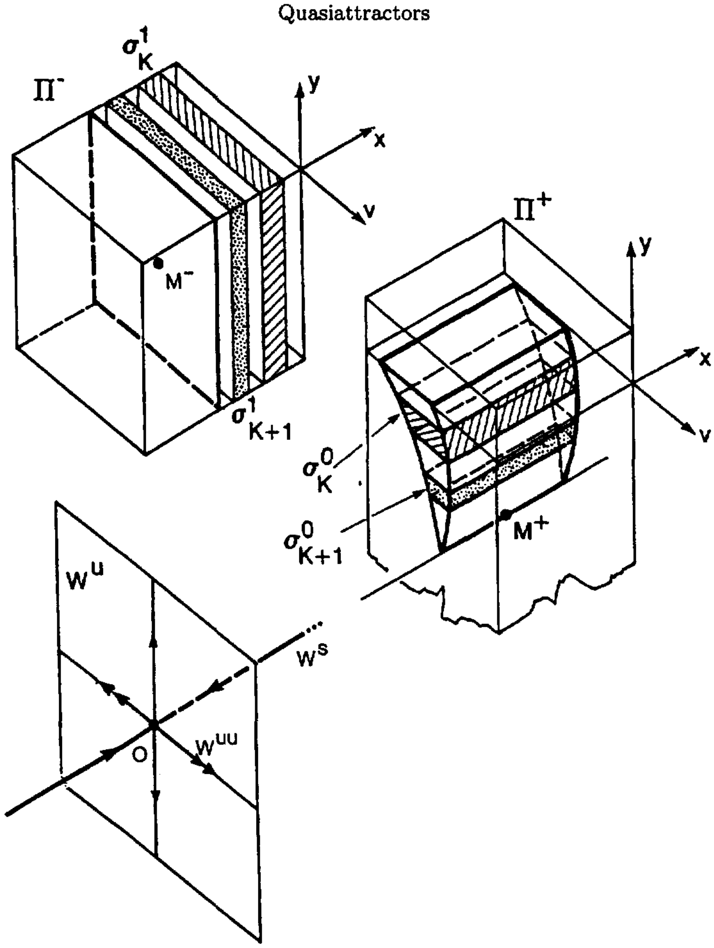

Figure 21. The three-dimensional case where the multipliers λ_1, γ_1, and γ_2 of the fixed point O are such that $0 < \lambda_1 < 1 < \gamma_1 \ll \gamma_2$. Here the strips $\sigma_k^1 \subset \Pi^-$ are three-dimensional "plates," accumulating on $W^u \cap \Pi^-$ as $k \to \infty$. The strips σ_k^0 lie in a wedge abutting $W^s \cap \Pi^+$, asymptotically contracted along the nonleading coordinate v and tangent to the leading plane $v = 0$ everywhere on $W^s \cap \Pi^+$.

written as

$$
\begin{aligned}
x_k &= A_1^k x_0 + \hat{\lambda}^k \xi_k(x_0, u_0, y_k, v_k),\\
u_k &= \hat{\lambda}^k \hat{\xi}_k(x_0, u_0, y_k, v_k),\\
y_0 &= B_1^{-k} y_k + \hat{\gamma}^{-k} \eta_k(x_0, u_0, y_k, v_k),\\
v_0 &= \hat{\gamma}^{-k} \hat{\eta}_k(x_0, u_0, y_k, v_k),
\end{aligned} \tag{4.14}
$$

where $\hat{\lambda}$ and $\hat{\gamma}$ are constants such that $0 < \hat{\lambda} < \lambda$, $\hat{\gamma} > \gamma$ and the functions $\xi_k, \hat{\xi}_k, \eta_k, \hat{\eta}_k$ are uniformly bounded at all k along with their derivatives up to the order $(r-2)$.

It is easily seen from these formulae that the points whose iterations approach a small neighborhood Π^- of some homoclinic point $M^- \in W^u_{\text{loc}}$ under the action of the map T_0, form a countable number of $(n+m)$-dimensional strips σ_k^0 in a small neighborhood Π^+ of some homoclinic point $M^+ \in W^s_{\text{loc}}$. For sufficiently large k, the strips σ_k^0 are strongly contracted along the v coordinate, while their images $\sigma_k^1 = T_0^k \sigma_k^0$ are contracted along the u coordinate (Figures 20 and 21). In the projection onto the leading coordinates, the strips will appear as shown in Figures 22–25. In the case of complex leading multipliers, the strips lie in involuted rolls which wind up, respectively, on the stable or the unstable manifold.

Using formulae (4.14), one can also calculate the first return maps $T_k : \sigma_k^0 \to \sigma_k^0$. In Case (1,1), there are no fundamental differences from the two-dimensional case due to the reduction theorem. The other cases are more complicated. Here, on most of the strips σ_k^0 there exist invariant

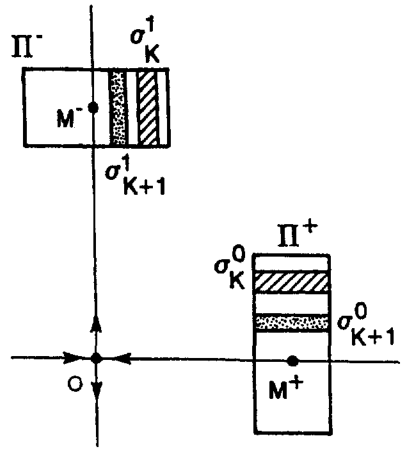

Figure 22. The projections of the multidimensional strips σ_k^0 and σ_k^1 on the leading plane $(u, v) = 0$ in Case (1,1). These projections look the same as in the two-dimensional case.

manifolds $\mathcal{M}_k$ on which the map T_k is close to the one-dimensional parabola map (see (3.1)), while along the directions complementary to such a manifold there is contraction or expansion that is stronger than on $\mathcal{M}_k$. The manifold $\mathcal{M}_k$ is not a global invariant manifold seizing all dynamics of the system in the neighborhood of the tangency, but it is an invariant manifold for the map T_k defined on the single strip σ_k^0. Nevertheless, the presence of these invariant manifolds allows one to reduce some questions to the study of two-dimensional maps $T_k|_{\mathcal{M}_k}$. In this way, the multidimensional version of Theorem 1 was proved in [30].

At the same time, there exists here a countable number of nonstandard strips, on which the map T_k is essentially multidimensional. Thus, if the product D of all the leading multipliers is less than unity, then for a countable number of strips σ_k^0 the first return map is close to one of maps given by formulae (3.2)–(3.4), for some rescaled coordinates (we write only that part of the map which corresponds to nontrivial behavior: for the other variables the map T_k acts as strong contraction or strong expansion).

We explain this statement in more detail for Case (2,1) at $D = \lambda^2\gamma < 1$ and $\lambda\gamma > 1$. For the sake of simplicity, we suppose that there are no nonleading multipliers; i.e., we consider the three-dimensional case where the multipliers of O are $\lambda_{1,2} = \lambda e^{\pm i\varphi}$ and γ (here $0 < \lambda < 1$, $\gamma > 1$).

LEMMA 3. *In the case under consideration, there exist infinitely many strips σ_k^0 for which the map T_k takes the form*

$$\begin{aligned} \bar{x}_1 &= x_1 + \varepsilon_{1k}(x_1, x_2, y), \\ \bar{x}_2 &= y + \varepsilon_{2k}(x_1, x_2, y), \\ \bar{y} &= M - y^2 - Bx_1 + \varepsilon_{3k}(x_1, x_2, y), \end{aligned} \tag{4.15}$$

in some rescaled coordinates. Here M and B are rescaled parameters which can take arbitrary finite values for k large enough; the functions ε_{ik} tend to zero as $k \to \infty$.

PROOF. By (4.12),(4.13), the map T_0 has the form

$$\begin{aligned} \bar{x}_1 &= \lambda(x_1 \cos\varphi - x_2 \sin\varphi) + O\left(\|x\|^2|y|\right), \\ \bar{x}_2 &= \lambda(x_2 \cos\varphi + x_1 \sin\varphi) + O\left(\|x\|^2|y|\right), \\ \bar{y} &= \gamma y + O\left(\|x\|\,|y|^2\right). \end{aligned} \tag{4.16}$$

Take a pair of homoclinic points $M^-(0, 0, y^-) \in W^u_{\rm loc}$ and $M^+(x_1^+, x_2^+, 0) \in W^s_{\rm loc}$. Since W^u and W^s have a quadratic tangency at M^+, the global map T_1 acting from a small neighborhood

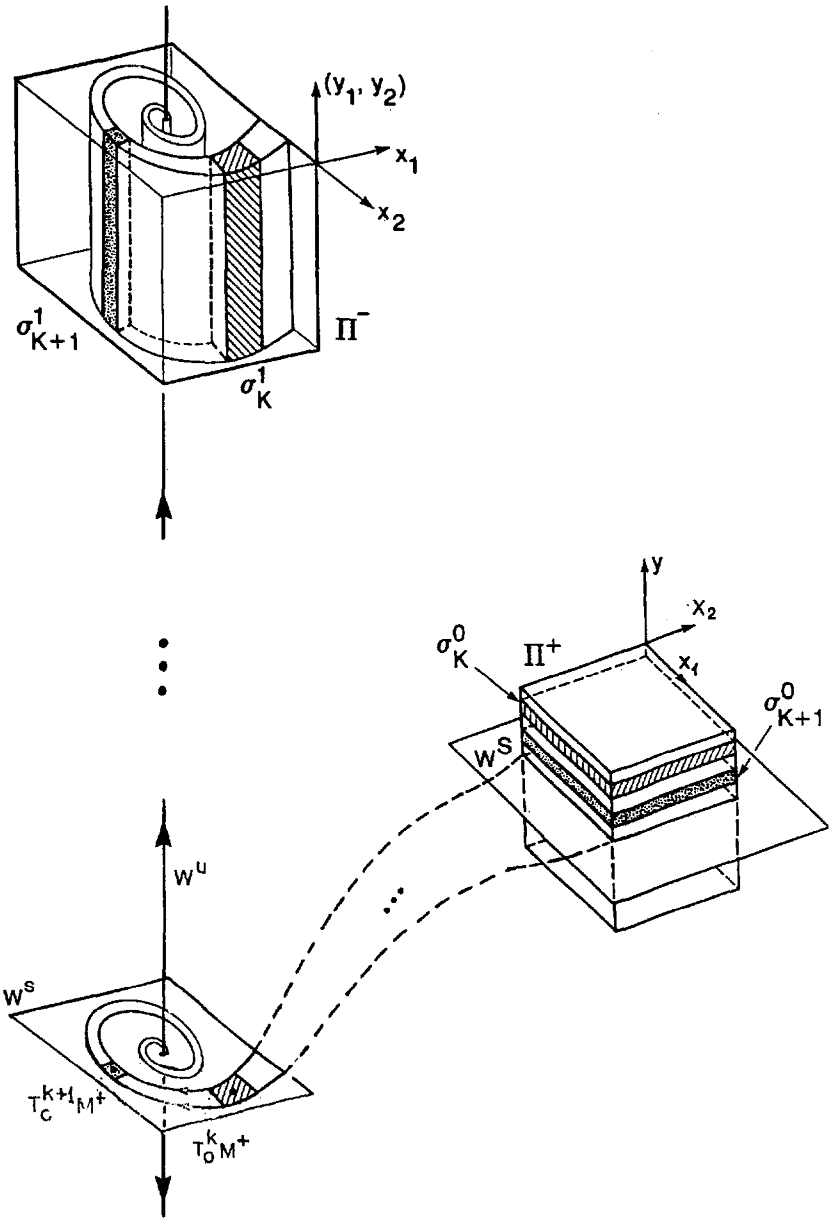

Figure 23. The three-dimensional strips σ_k^0 and σ_k^1 in Case (2,1), where the fixed point O has multipliers 0 $\lambda_{1,2} = \lambda e^{\pm i\varphi}$ and $\gamma_1 > 1$. Here the strips $\sigma_k^0 \subset \Pi^+$ are three-dimensional "plates" accumulating on $W^s \cap \Pi^+$ as $k \to \infty$. The strips σ_k^1 lie in the involuted roll, wound onto the segment $W^u \cap \Pi^-$.

of M^- into a small neighborhood of M^+, has the form

$$\begin{aligned} \bar{x}_1 - x_1^+ &= b_1(y - y^-) + a_{11}x_1 + a_{12}x_2 + \cdots, \\ \bar{x}_2 - x_2^+ &= b_2(y - y^-) + a_{21}x_1 + a_{22}x_2 + \cdots, \\ \bar{y} &= \mu + c_1x_1 + c_2x_2 + d(y - y^-)^2 + \cdots, \end{aligned} \tag{4.17}$$

where $b_1^2 + b_2^2 \neq 0$, $c_1^2 + c_2^2 \neq 0$ since T_1 is a diffeomorphism, and $d \neq 0$ since the tangency is quadratic; μ is the splitting parameter.

We may assume $b_1 \neq 0$. By the orthogonal coordinate transformation

$$x_1 \to x_1 \cos\alpha + x_2 \sin\alpha, \qquad x_2 \to x_2 \cos\alpha - x_1 \sin\alpha,$$

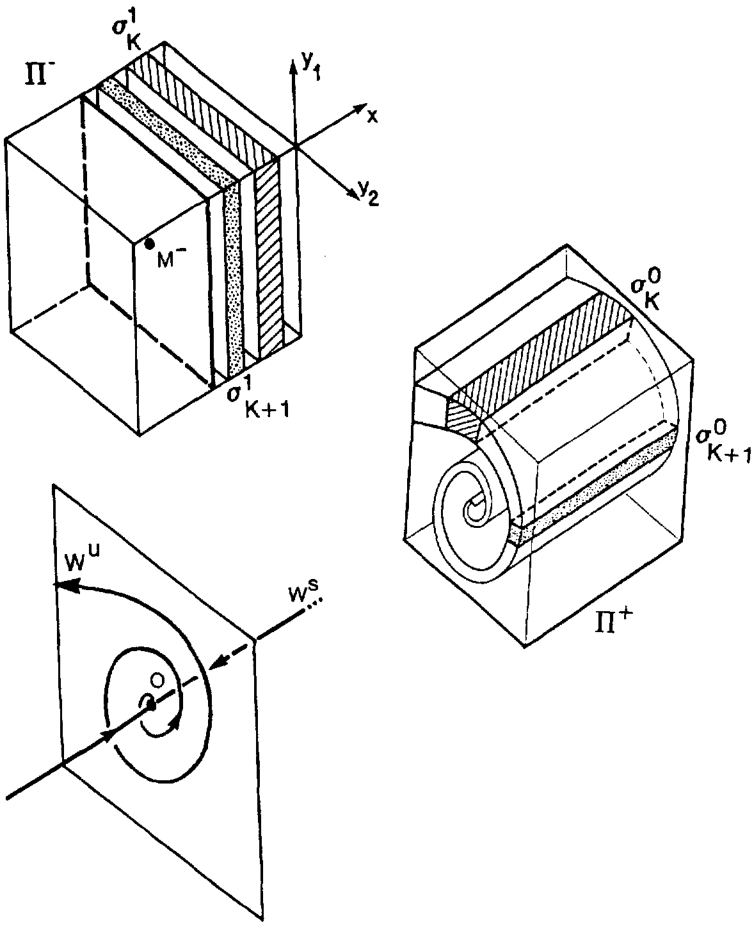

Figure 24. The three-dimensional strips σ_k^0 and σ_k^1 in Case (1,2), where the fixed point O has multipliers $0 < \lambda_1 < 1$ and $\gamma_{1,2} = \gamma e^{\pm i\varphi}$. Here the strips $\sigma_k^1 \subset \Pi^-$ are three-dimensional "plates" accumulating on $W^u \cap \Pi^-$ as $k \to \infty$. The strips σ_k^0 lie in the involuted roll, wound onto the segment $W^s \cap \Pi^+$.

that obviously do not change form (4.16) of the local map, the term $b_2(y - y^-)$ in the second equation of (4.17) can be eliminated if $b_2 \cos\alpha - b_1 \sin\alpha = 0$, and the global map takes the form

$$\begin{aligned} \bar{x}_1 - x_1^+ &= b(y - y^-) + a_{11}x_1 + a_{12}x_2 + \cdots , \\ \bar{x}_2 - x_2^+ &= a_{21}x_1 + a_{22}x_2 + \cdots , \\ \bar{y} &= \mu + c_1x_1 + c_2x_2 + d(y - y^-)^2 + \cdots , \end{aligned} \tag{4.18}$$

with new coefficients x_i^+, a_{ij}, c_i. Here $b \neq 0$, and still $c_1^2 + c_2^2 \neq 0$.

By (4.14),(4.18), the first return map $T_k = T_1T_0^k$ is written in the form

$$\begin{aligned} \bar{x}_1 - x_1^+ &= b(y - y^-) + a_{11}\lambda^k x_1 + a_{12}\lambda^k x_2 + \cdots , \\ \bar{x}_2 - x_2^+ &= a_{21}\lambda^k x_1 + a_{22}\lambda^k x_2 + \cdots , \\ \gamma^{-k}(\bar{y} - y^-) + \gamma^{-k}y^- + \hat{\gamma}^{-k}\eta_k(\bar{x}, \bar{y}) &= \mu + \lambda^k\beta_{1k}(\varphi)x_1 + \lambda^2\beta_{2k}(\varphi)x_2 \\ &\quad + d(y - y^-)^2 + \cdots , \end{aligned} \tag{4.19}$$

where $\beta_{1k}(\varphi) = c_1 \cos k\varphi + c_2 \sin k\varphi$, $\beta_{2k}(\varphi) = c_2 \cos k\varphi - c_1 \sin k\varphi$.

Shifting the origin: $y \to y + y^-$, $x \to x + x^+ + \cdots$, we can eliminate the constant terms in the first two equations of (4.19) and the map takes the form

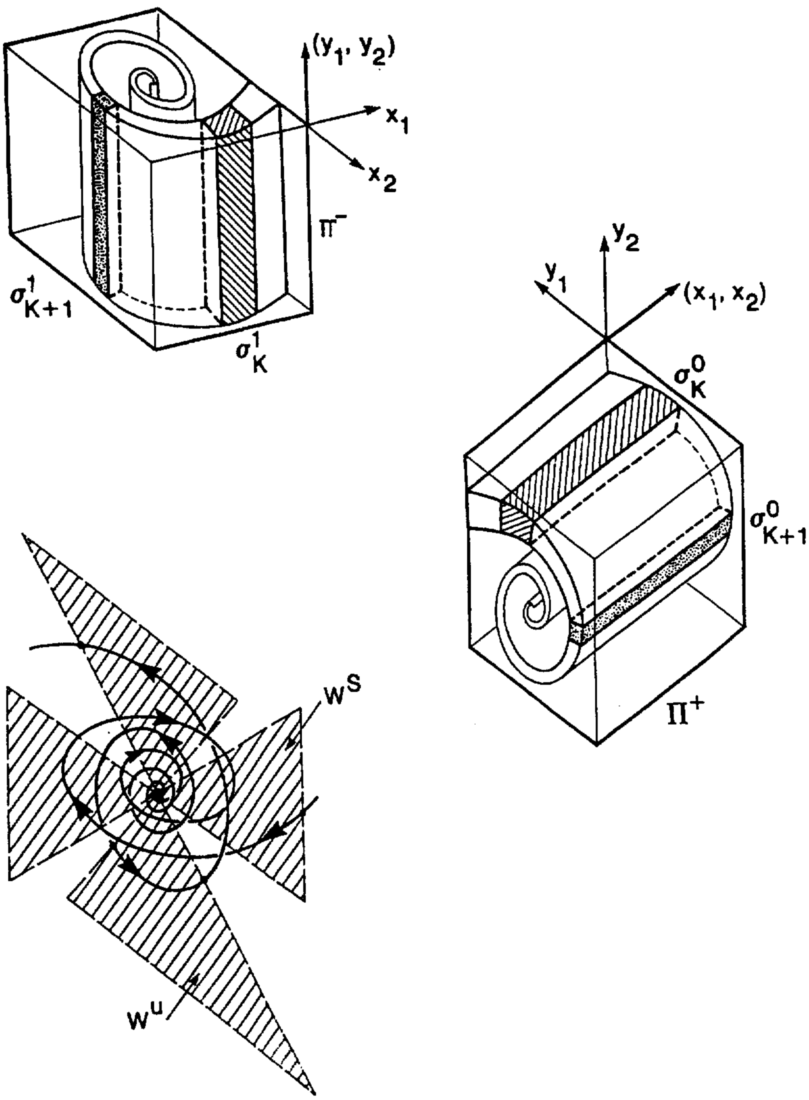

Figure 25. The four-dimensional strips σ_k^0 and σ_k^1 in Case (2,2), where the fixed point O has multipliers 0 $\lambda_{1,2} = \lambda e^{\pm i\varphi}$ and $\gamma_{1,2} = \gamma e^{\pm i\psi}$. Here the strips $\sigma_k^1 \subset \Pi^-$ lie in the involuted roll wound onto the two-dimensional area $W^u \cap \Pi^-$. The strips σ_k^0 lie in the involuted roll, wound onto the $W^s \cap \Pi^+$.

$$
\begin{aligned}
\bar{x}_1 &= by + \lambda^k O\left(\|x\|\right) + O\left(y^2\right), \\
\bar{x}_2 &= a_{21}\lambda^k x_1 + a_{22}\lambda^k x_2 + O\left(y^2\right) + \lambda^k o\left(\|x\|\right), \\
\bar{y} + \left(\frac{\hat{\gamma}}{\gamma}\right)^{-k} O\left(|\bar{y}| + \|\bar{x}\|\right) &= M_1 + d\gamma^k y^2 + (\lambda\gamma)^k \beta_{1k}(\varphi) x_1 + (\lambda\gamma)^k \beta_{2k}(\varphi) x_2 \\
&\quad + \lambda^k \gamma^k O\left(\|x\|^2 + |y| \cdot \|x\|\right) + \gamma^k o(y^2),
\end{aligned}
\tag{4.20}
$$

where

$$
M_1 = \gamma^k \left(\mu + \lambda^k \beta_{1k}(\varphi)\xi_1^+ + \lambda^k \beta_{2k}(\varphi)\xi_2^+ - \gamma^{-k} y^- + \cdots\right).
$$

Rescaling the variables

$$
x_1 \to -\frac{b}{d} x_1 \gamma^{-k}, \qquad x_2 \to -\frac{b}{d} a_{21} x_2 \lambda^k \gamma^{-k}, \qquad y \to -\frac{1}{d} y \gamma^{-k},
$$

we get the following expression for the map T_k:

$$\begin{aligned} \bar{x}_1 &= y + \cdots , \\ \bar{x}_2 &= x_1 + \cdots , \\ \bar{y} &= M - y^2 - Bx_1 + \left(\lambda^2\gamma\right)^k \beta_{2k}(\varphi)x_2 + \cdots , \end{aligned} \tag{4.21}$$

where the dots stand for the terms which tend to zero as $k \to \infty$; $M = -d\gamma^k M_1$, $B = -b\beta_{1k}(\varphi)(\lambda\gamma)^k$.

Recall that we consider the case $\lambda\gamma > 1$, $\lambda^2\gamma < 1$. Therefore, $(\lambda^2\gamma)^k \ll 1$ and $(\lambda\gamma)^k \gg 1$ at large k. Thus, the term with x_2 in the third equation of (4.21) is small, so the map is now brought to form (4.15). The coefficient B is the product of the large quantity $(\lambda\gamma)^k$ and the value $\beta_{1k} = c_1 \cos k\varphi + c_2 \sin k\varphi$. When the ratio $\frac{\varphi}{\pi}$ is abnormally (exponentially) well approximated by rational fractions (such φ are dense on the interval $(0, \pi)$), the coefficient β_{1k} can be made appropriately small for a countable number of values of k, so that B may take an arbitrary finite value. The lemma is proved.

REFERENCES

1. I.M. Ovsyannikov and L.P. Shil'nikov, *Math. Sbornik* **58** (1987).
2. I.M. Ovsyannikov and L.P. Shil'nikov, *Math. Sbornik* **73** (1992).
3. L.P. Shil'nikov, *Selecta Math. Sovietica* **10** (1991); Originally published in *Methods of Qualitative Theory of Differential Equations*, (in Russian), Gorki University Press, (1986).
4. L.P. Shil'nikov, *Sov. Math. Dokl.* **6** (1965).
5. L.P. Shil'nikov, *Math. Sbornik* **10** (1970).
6. V.S. Afraimovich and L.P. Shil'nikov, *Amer. Math. Soc. Trans.* **149** (2) (1991); Originally published in *Methods of Qualitative Theory of Differential Equations*, (in Russian), Gorki University Press, (1983).
7. D.V. Turaev and L.P. Shil'nikov, *Mathematical Mechanisms of Turbulence*, (in Russian), Ukrainian Math. Institute, (1986).
8. V.S. Afraimovich and L.P. Shil'nikov, *Sov. Math. Dokl.* **24** (1974).
9. S.E. Newhouse, J. Palis and F. Takens, *Publ. Math. Inst. Haute Etudes Scientifiques* **57** (1983).
10. L.O. Chua, M. Komuro and T. Matsumoto, Parts 1 and 2, *IEEE Trans. Circuits Syst.* **CAS-33** (1986).
11. L.P. Shil'nikov, *Int. J. of Bifurcation and Chaos* 4 (3) (1994).
12. M. Henon, *Comm. Math. Phys.* **50** (1) (1976).
13. M. Benedicks and L. Carleson, *Ann. of Math.* **133** (1991).
14. Y.C. Lai, C. Grebogi, J.A. Yorke and I. Kan, *Nonlinearity* **6** (1993).
15. V.S. Afraimovich, V.V. Bykov and L.P. Shil'nikov, *Uspekhi Mat. Nauk* (in Russian) **36** (4) (1980).
16. A.L. Shil'nikov and L.P. Shil'nikov, *Int. J. of Bifurcation and Chaos* **1** (1991).
17. V.V. Bykov and A.L. Shil'nikov, *Selecta Math. Sovietica* **11** (1992); Originally published in *Methods of Qualitative Theory of Differential Equations*, (in Russian), Gorki University Press, (1989).
18. P. Holms, *Philos. Trans. Roy. Soc.* **A292** (1979).
19. J. Ueda, *J. Statist. Phys.* **20** (4) (1979).
20. A.S. Dmitriev, Yu.A. Komlev and D.V. Turaev, *Int. J. of Bifurcation and Chaos* **2** (1) (1992).
21. A.D. Morozov and L.P. Shil'nikov, *J. Appl. Math. and Mech.* (in Russian) **47** (1983).
22. V.S. Afraimovich and L.P. Shil'nikov, *Nonlinear Dynamics and Turbulence*, (Edited by G.I. Barenblatt, G. Iooss, D.D. Joseph), Boston, Pitmen, (1983).
23. R. Mane, *Publ. Math. Inst. Haute Etudes Scientifiques* **66**, 139–159 (1988).
24. R. Mane, *Publ. Math. Inst. Haute Etudes Scientifiques* **66**, 161–210 (1988).
25. S. Smale, *Differentiable and Combinatorial Topology*, (Edited by S.S. Cairns), Princeton University Press, (1963).
26. L.P. Shil'nikov, *Math. USSR Sb.* **3** (1967).
27. N.K. Gavrilov and L.P. Shil'nikov, Part 1, *Math. USSR Sb.* **17** (1972).
28. N.K. Gavrilov and L.P. Shil'nikov, Part 2, *Math. USSR Sb.* **19** (1973).
29. S.E. Newhouse, *Publ. Math. Inst. Haute Etudes Scientifiques* **50** (1979).
30. S.V. Gonchenko, L.P. Shil'nikov and D.V. Turaev, *Russian Acad. Sci. Dokl. Math.* **47** (2) (1993).
31. J. Palis and M. Viana, High-dimension diffeomorphisms displaying infinitely many sinkc, *IMPA* (preprint) (1992).
32. S.V. Gonchenko, L.P. Shil'nikov and D.V. Turaev, *Soviet Math. Dokl.* **44** (1992); Originally published: *Dokl. Akad. Nauk. SSSR*.
33. S.V. Gonchenko, L.P. Shil'nikov and D.V. Turaev, *Physica D* **62**, 1–4 (1993).
34. L. Tedeschini-Lalli and J.A. Yorke, *Commun. Math. Phys.* **106** (1986).

35. S.E. Newhouse, *Topology* **12** (1974).
36. S.V. Gonchenko, L.P. Shil'nikov and D.V. Turaev, *Russian Acad. Sci. Dokl. Math.* **47** (3) (1993).
37. M.W. Hirsh, C.C. Pugh and M. Shub, *Lecture Notes in Math.* **583** (1977).
38. A.L. Shil'nikov, L.P. Shil'nikov and D.V. Turaev, *Int. J. of Bifurcation and Chaos* **3** (5) (1993).
39. A. Arneodo, P.H. Collet, E.A. Spiegel and C. Tresser, *Physica D* **14** (1985).
40. J. Kaplan and J. Yorke, *Lecture Notes in Math.* **730** (1979).
41. S.V. Gonchenko and L.P. Shil'nikov, *Ukrainian Math. J.* **42** (2) (1990).
42. S.V. Gonchenko and L.P. Shil'nikov, *Russian Acad. Sci. Izv. Math.* **41** (3) (1993); Originally published in Izvestia Rossiyskoi Akademii Nauk, *Seria Matem,* **56** (6) (1992).
43. S.V. Gonchenko, *Methods of Qualitative Theory of Differential Equations*, (in Russian), Gorki Univ. Press, (1984).
44. S.V. Gonchenko and L.P. Shil'nikov, *Ukrainian Math. J.* **39** (1987).
45. S.V. Gonchenko and L.P. Shil'nikov, *Soviet. Math. Dokl.* **33** (1986).